Bull. Disas. Prev. Res. Inst., Kyoto Univ., Vol. 34, Part 3, No. 307, September, 1984

On a Formation Mechanism of Topography and Its Relation to Earthquake Occurrence in Southwest Japan

By Kazuo MINO

(Manuscript received June 30, 1984)

Abstract

Topography and earthquake occurrence in Southwest Japan were analysed in detail to investigate their formation mechanism.

Two methods were applied to analyse topography. One is a two-demensional Fourier analysis and the other is a band-pass filtering. The data used here are the mean elevation published by the Geographical Survey Institute of Japan, which are represented by the mesh data in a unit rectangle of 1.5' and 1' along longitude and latitude, respectively.

The results of the two-dimensional Fourier analysis indicate that a wavelength of about 40 km appears to be a boundary value corresponding to relatively wide areas, wavelengths longer than 40 km are observed over all regions, and those shorter than 40 km show large locality.

Seya's band-pass filtering was applied, referring to the results of the two-dimensional Fourier analysis. Extracted topography is classified into those with long, intermediate and short wavelengths. There exist two predominant topographies with long wavelengths (70–150 km). One is that with an EW strike in the Chugoku and Shikoku districts, another with an NS strike in the Chubu district. In the range from short and intermediate wavelengths, the topography in the Chubu region and the Outer Zone in Southwest Japan shows rather regular pattern being approximately the same as that with the long wavelengths, but the detailed topographies with short and intermediate wavelengths are more complicated in the Chugoku and Kinki districts.

It appears that the upper crust in the Chugoku and Kinki districts may be divided into quadrilaterals probably due to double foldings by NS and EW compressions and bordered by faults of strike-slip type. Boundaries of these crustal blocks are considered as relatively wide crushed zones which were probably produced by block motions.

Large earthquakes are mostly located on the boundaries between uplift and subsidence areas of the fold, which may correspond to the faults caused by the development of the fold.

Microearthquake distribution appears to have a close relation to the topography with long wavelengths and, on the other hand, to that with very short wavelengths as well. These two phenomena are owing to extremely frequent occurrence and very small source dimensions of microearthquakes. Rivers and sharp notches often appear related to microearthquake distribution. This shows that these fine structures are manifestations on the surface of the present stress acting in the crust.

All of these features of topography in Southwest Japan are fundamentally explained by two compressions in EW and NS directions by subductions of the Pacific plate and Philippine Sea plate which have continued since the late Quaternary.

The present tectonic stress, which is considered to be an extension of that from the geological times, still causes not only the formation of the topography but crustal activity including earthquake occurrence.

1. Introduction

Topography is built up by two kinds of deformations. One is the deformation such as uplift, subsidence and break which are caused by the endogenic force in the Earth's interior. The other is that by the exogenic agency such as erosion. However, if we are mainly concerned with topographies with considerably long dimensions such as large mountains, the former agency may have much more fundamental effects on those topographies, particularly in areas with high tectonic activity such as Japan Islands.

On the other hand, geophysical phenomena in the Earth's crust including earthquakes and crustal movements have been considered to be manifestations only of the present state of tectonics. In spite of the important problem, the relation between such geophysical phenoemna and topographical ones has yet been fully treated.

Recently, however, it has been mentioned some times[1),2)] that earthquake occurrence, for instance, is related to the present topography which has been making for a long time, probably since the late Quaternary. This means that present crustal activities should be considered on the extension of the tectonic movement since the late Quaternary period, and that such investigations will bring about essential understanding of the formation of the topography and crustal activities.

In this paper, from the above point of view, we shall analyse present topography in Southwest Japan and investigate the formation mechanism of topography and its relation to seismic activity. First, a brief review of research works on topography, mainly on fold and fault topographies, will be given.

Studies of geomorphology in Japan, were commenced at the end of the 19th century, when Davis[3)] proposed a geomorphic cycle theory which is an idealized model of erosion. This theory has been introduced and prevailing also in Japan. Tujimura[4)] published "Geomorphology" (in Japanese), which was based on the concept of Davis[3)], and he explained this theory by using a plenty of examples of topographies in Japan. Moreover, he suggested to consider the force of formation of topography, which is not only exogenic force but endogenic one.

Otsuka[5)] proposed the existence of an active fold on the basis of the distribution of altitudes of river terrace. The deformation of an active fold was also confirmed by Sugimura[6)] by geologiacl and leveling surveys on a terrace along the Oguni river. He also recognized that the deformation of altitudes of the terrace consisted with geological structure and that the older surface of the terrace had suffered larger deformations.

Kaizuka[7)] investigated deformation of folds, and derived that time rate of deformation is generally inversely correlated with wavelength. He also estimated the deformation of folding block as 10^{-2} in a block with 15–16 km in length and 5–6 km in width, and as 10^{-3} in a block with 30–60 km in length and 10–20 km width, and this inverse correlation holds good up to 100 km. This correlation was also confirmed by Matsuda[8)] and Ota[9)].

Kaizuka[7] also showed that the velocity of development of a fold in the Quaternary period agrees with that of the presnet deformation derived from leveling surveys[10].

Kaizuka[11] asserted that a fold in the Quaternary preiod has developed in the same stress field as that generating earthquakes at present.

Miyamura and Mizoue[10] analysed the modes of the present crustal movements in different tectonic areas in several time spans on the basis of results of leveling surveys. They also discussed tectonic activities in Japan and concluded that low activity of crustal movement was found in Southwest Japan and the Outer Zone of Northeast Japan. The velocity of deformation of the active fold was estimated to be $1\text{–}3\times10^{-6}$/yr by leveling surveys[12].

Yoshikawa[13] proposed that classification of active blocks according to wavelengths and its regional property should be investigated. He showed that a pattern of the vertical displacements in the Quaternary period has a prevailing wavelength of 200 km, and that this pattern is vrey similar to the present configuration of Japan Islands.

Fault topography has also been investigated. A seismic fault associated with a large earthquake attracted the attention of geomorphologists, geologists and geophysicists. One of the most important contributions in the investigations on the seismic fault was derived by Kuno[14]. He stated that the Tanna fault moved about 3.5 m in lateral and 1.5 m in vertical directions at the Kita Izu Earthquake, M: 7.0 in 1930, and that the distribution of pattern of the coseismic displacement over some area was similar to that in recent geological time. His study has also revealed that an active fault displaces in a constant direction and the displacements are accumulated. Matsuda[15] made detailed geological and geomorphological survey on the Atotsugawa fault in central Japan, and confirmed that the fault topography is the result of accumulation of the displacements caused by successive earthquakes on the basis of the evidence that the older rivers and valleys crossing the fault have large lateral displacements. He also stated that this fault has been developed in the Quaternary period, judging from small deformation of rock materials in the Tertiary period.

Sugimura and Mtasuda[16], studying the Atera fault in central Japan, found in an area where the Atera fault intresects the Kiso river that some terraces belonging to different epochs in the Quaternary showed different displacements. They attempted to infer displacements of the terraces from the old state of the fault and concluded the Atera fault has moved from the beginning of the Quaternary up to the present.

The Median Tectonic Line (hereafter called MTL) is the largest fault in Japan, running across Southwest Japan from east to west. It was recognized as an active fault having the right lateral strike-slip, uplifting on its northern side, and a high dislocation velocity of 4–5 mm/yr[17),18)]

Huzita et al[19]. mentioned that activity of microearthquakes is high along the boundary of geological blocks which is usually formed by an active fault and tectonic line.

Matsuda[20] proposed a formula indicating a relation between the magnitude and the fault length, and suggested the recurrence interval of earthquakes. The knowledge about the recurrence interval of large earthquakes is very important not only for earthquake prediction but for the history of land formations. Most investigations cited above are based on the observations of topography itself and geological phenomena related to it, and its process of formation was derived therefrom. Systematic analyses of dimensions of topography, however, are not considered to have been sufficiently treated. In the present study the topography will be analysed from the viewpoints of wavelength and spatial distribution of topography, and formation mechanism of topography will be discussed based on these results. Thus, in the following, the method and result of analysis of topography in Southwest Japan will be described in the second chapter. In the third and fourth chapters, topographies with long and short wavelength will be treated, respectively, and the formation mechanisms of these topographies will be discussed. In the fifth chapter, the structure of an active fault as the boundary of two topographies will be shown. And in the last chapter, the relation between topography and earthquake occurrence will be mentioned.

2. Analysis of topography

2.1. Data

(1) Topography data

Topography is described by the elevation of land. Such data are published by the Geographical Survey Institute of Japan, and represented by a mean value of elevations measured in 10 m unit in a certain unit area. The unit area is a rectangle enclosed by 1′ along longitude and 1.5′ along latitude. These lengths are about 1.85 and 2.25 km at 35° N, respectively. A geographical map of 1/200,000 scale is composed of 40×40 parts with this unit area. The Japan Islands are composed of 111 sheets of the geographical map of 1/200,000 scale, which are numbered as shown in **Fig. 1**.

(2) An outline of Southwest Japan

As shown in **Fig. 2**, the Japan Islands may be divided geologically into two regions by the Itoigawa-Shizuoka Line (hereafter called ISL), which is the west edge of the Fossa Magna. The area west of the ISL is called Southwest Japan, which is also sub-divided into two parts by the MTL. The area south of the MTL is called the Outer Zone and the northern area the Inner Zone. The Inner Zone may be tentatively divided three areas by two tectonic lines. One of them is the Tsuruga-Ise bays line (hereafter called TIL) which divide the Kinki district from the Chubu mountainous region. Another is the Yura-Kako rivers line (hereafter called YKL) which is the largest trough which divide the Kinki area from the Chugoku mountainous region. Then the Chubu district is located between the ISL and the TIL and the western area of the YKL is called the Chugoku district.

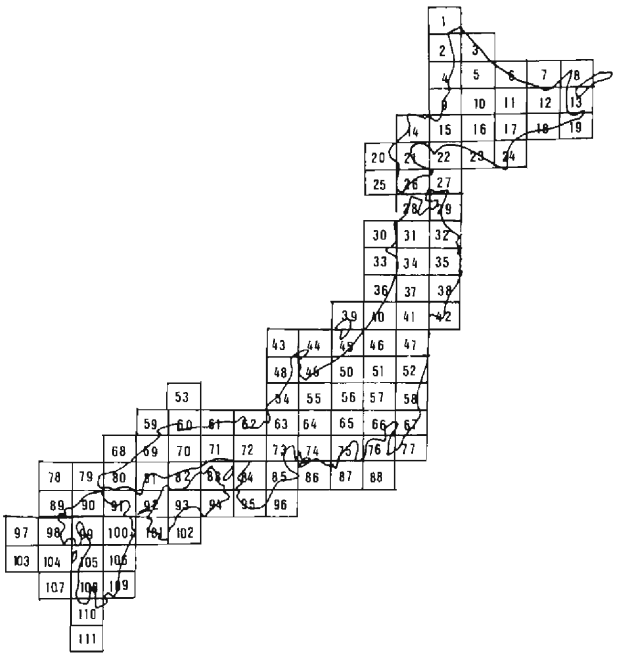

Fig. 1 Numbering of 1/200,000 scale topographic maps published by the Geographical Survey Institute of Japan

Numerals in **Fig. 2** indicate mountainous area and letters, A-F, indicate rivers, channels and bays. Contours indicate 100, 400 (heavy line), 600 and 1,000 m, respectively.

2.2. 2-dimensional Fourier analysis

(1) 2-dimensional Fourier method[21)]

First, we shall apply a 2-dimensional Fourier analysis to detect predominant wavelengths of topography in each sub-divided region of Southwest Japan.

Data array is indicated by $a_{m\Delta x,n\Delta y}$, where Δx and Δy are unit lengths in the X and Y directions, respectively, and $m=0, 1, 2, \cdots, M-1$, $n=0, 1, 2, \cdots, N-1$. Fourier transform of $a_{m\Delta x,n\Delta y}$ is expressed as follows:

$$A_{u\Delta x,v\Delta l} = \sum_{m=0}^{M-1}\sum_{N=0}^{N-1} a_{m\Delta x,n\Delta y} \exp\{-2\pi i(m\Delta x \cdot u\Delta k + n\Delta y \cdot v\Delta l)\}\Delta x\Delta y \qquad (2\text{–}1)$$

where, $i=\sqrt{-1}$, $k=1/M\Delta x$, $1=1/N\Delta y$, and $A_{u\Delta k,v\Delta l}$ is expressed in length units. The following weight function was applied before the calculation of the Fourier transform, for the sake of smoothing data,

$$\omega(i,j) = \sqrt{(-\cos i+1.0)\cdot(-\cos j+1.0)}/2.0 \qquad (2\text{–}2)$$

where, $i=m'\Delta x$ and $j=n'\Delta y$ depend both on data and frequencies. In the present analysis, all components of wavelengths shorter than 10 km have been neglected.

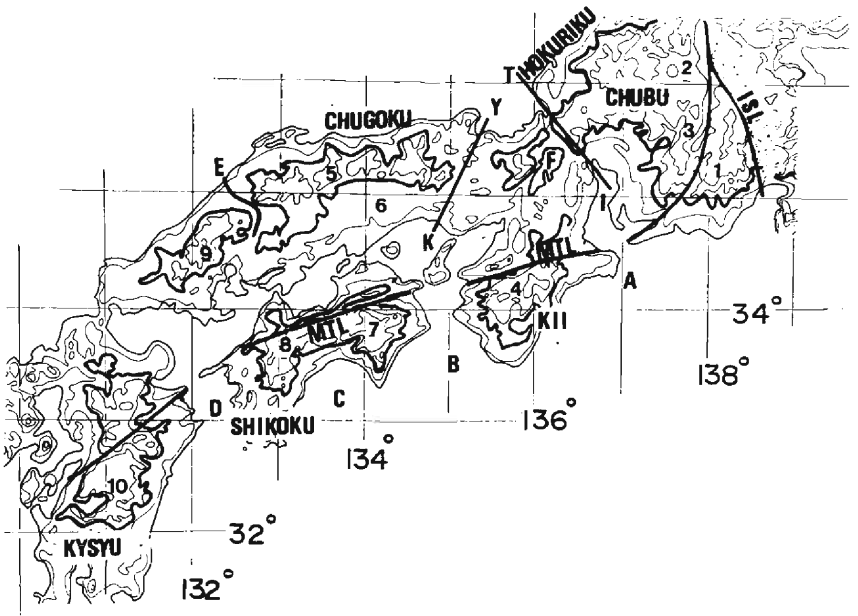

Fig. 2 The features of topography of Southwest Japan
ISL : Itoigawa-Shizuoka line
MTL: Median Tectonic Line
YKL : Yura-Kako rivers line (Y–K)
TIL : Tsuruga-Ise bays line (T–I)
A: Ise bay, B: Kii channel, C: Tosa bya, D: Bungo channel, E: Go river, F: Lake Biwa
1: Akaishi mountains, 2: Hida mountains, 3: Kiso mountains, 4: Kii mountains, 5: Chugoku mountains, 6: Setouchi peneplain, 7: Eastern Shikoku mountains, 8: Western Shikoku mountains, 9: Kanmuriyama mountains, 10: Kyushu mountains.

(2) Two examples

We will show two smiple examples of analysis in order to facilitate understanding the results. The first testing model is a box-shaped topography with side-lnegth of 20 km (R=10 km) and a height of 1 km, as hsown in **Fig. 3**. The horizontal axis indicates the wavelength of topographies in km produced by horizontal compression in the NS direction. The vertical axis indicates, in the same manner, the wavelength in the case of horizontal compressoin in the EW direction. Wavelengths over 20 km are not usable and are cut off from the graph as shown by hatched areas. The graph indicates a symmetrical pattern, which is caused by the symmetrical shape of the model. The dominant wavelength is 16 km both in the NS and EW directions. Considering the accuracy of analysis, this value, 16 km, corresponds approximately to 20 km which is the side-length itself of the model. The next significant value of wavelength 10.3 km which is close to 10 km might be regarded as a reasonable value as the second mode.

The second testing model is shown in **Fig. 4**. The dimension of the model is the same as the first one, but it has valleys with a strike trending in the EW direction and a width of 2 km. The solution is shown at the lower part of **Fig. 4**.

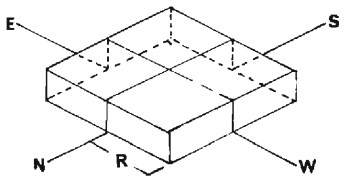

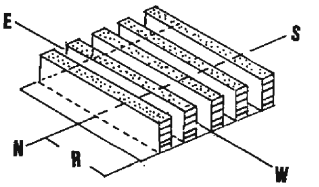

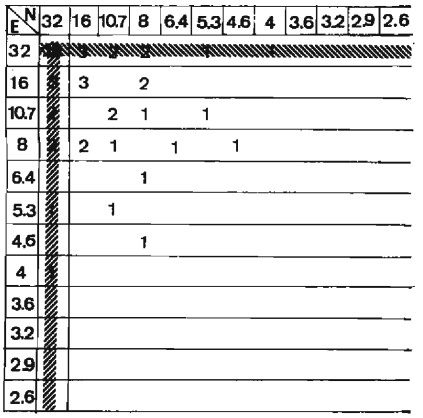

Fig. 3 Upper: the shape of the first model for the 2-dimensional Fourier analysis
Lower: the 2-dimensional spectra

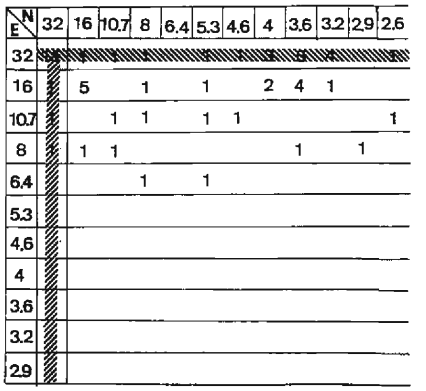

Fig. 4 Upper: the shape of the second model
Lower: the 2-dimensional spectra

In this case a dominant and significant value is found to be only at 3.6–4.0 km along the horizontal axis, which is produced by NS compression, and consists with the expected value, 4.0 km.

(3) Results of analysis

We have applied the 2-dimensional Fourier analysis to the mesh data described in 2.1, in order to know rough characteristics regarding topographic wavelength in each region. To do so, it is necessary to estimate the dimension of the area applied by the above method.

A relation between the magnitude of an earthquake and the length of the fault associated with the earthquake was given by Matsuda[20], as follows:

$$\log L = 0.6M - 2.9 \qquad (2\text{–}3)$$

The magnitude (M) of large and disastrous earthquakes being 6.0–7.5, it follows that lengths (L) of the faults are in a range between 5–40 km. According to Kaizuka[11], the dimension of one deformed block measured baout 15–100 km. Considering these dimensions, a region composed of 4 sheets of the geographical map of 1/200,000 scale was adopted for each analysis. This area is a rectangle with dimensions of 2 degrees along latitude and 1 degree and twenty minutes along

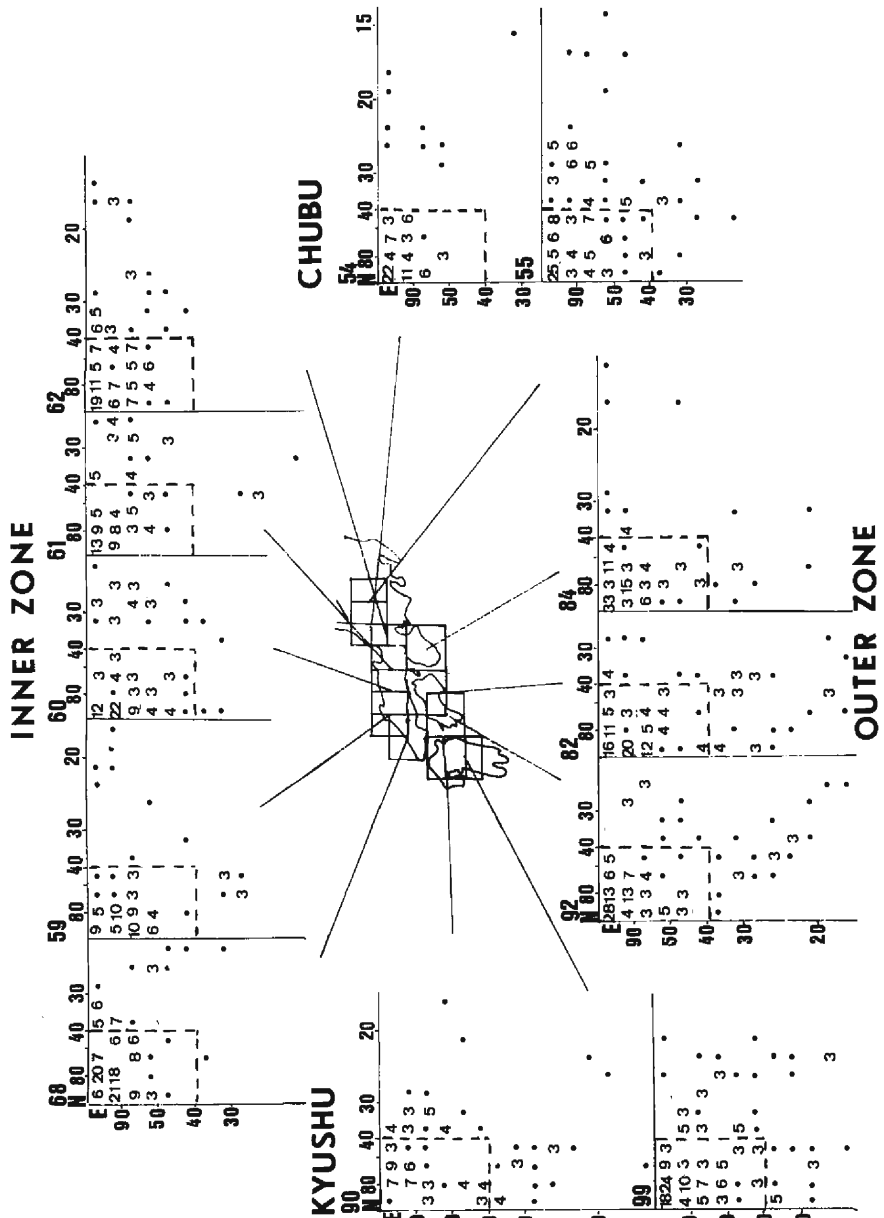

Fig. 5 The result of the 2-dimensional Fourier analysis in each region, classified into 4 groups which are the Inner Zone, the Outer Zone, the Kyushu and Chubu districts.
Dotted line indicates a presumed boundary of wavelength of 40 km between short and long wavelengths. Dots indicate the spectral values of 2.1 and smaller values are neglected as noise.

longitude. A typical length of this area is about 200 km, so that the significant wave-lengths deduced from the analysis should be shorter than 100 km.

An area composed of 4 sheets is called here by the index attached to the north-west-most sheet. For instance, No. 84 represents the area composed of 84, 85, 95 and 96 shown in **Fig. 1**. In practical calculations, Δx and Δy in $M\Delta x$ and $N\Delta y$ in equation (2–1) are taken as 2.25 and 1.85 km, respectively.

The results of analysis are presented in **Fig. 5**, which are classified into four groups, the Inner Zone, Outer Zone, Chubu and Kyushu. In each 2-dimensional spectrum, spectral amplitudes of 2 are indicated by dots and those of 1 or smaller have been omitted as noise. Units of spectrum were described in 10 m unit. The wavelength of 40 km in the EW and NS directions is shown by dotted lines, because this wavelength seems to be a certain boundary between long and short wavelengths. From the figure, the following spectral features may be noticed:

1. Wavelengths longer than 40 km both in the NS and EW directions commonly exist in all areas.
2. In the Outer Zone, some wavelengths longer than 40 km in the NS direction and shorter than 40 km in the EW direction exist. This means the existence of a topography slender in the NS direction, and we will call it "NS stripes" hereafter.
3. In the Inner Zone, on the contrary, the EW stripes are dominant, namely, longer than 40 km in the EW direction and shorter than 40 km in the NS direction. Also, a short wavelength, say, 30 km, in the EW direction can be seen in some areas.
4. In the Chubu and Kyushu districts, topographies show complicated features as to their directions compared with the Inner Zone and Outer Zone, but we can recognize wavelengths shorter than 40 km.
5. It can be said that the wavelength of about 40 km as a boundary in the spectral graph plays a major role to distinguish regional features, and that as for wavelengths shorter than 30 km, the regional differences are very large and there are no short wavelengths common in a wide area.

In order to discuss in detail the tectonics in these areas, however, it is necessary to consider together not only the above results derived from the spectral analysis but also those from some other kinds of treatments.

2.3. Analysis by band-pass filters

According to the 2-dimensional Fourier analysis of topography, the intermediate and short wavelengths indicate the specific characteristics in Southwest Japan. Predominant wavelengths are 40–60 and 20–30 km. In order to extract these characteristics of topography, we use a band-pass filter designed by Seya[22] for gravity prospecting. We will briefly describe the method of the Seya's filter.

(1) The Seya's filter

This filter is composed of two filters of running averages. The filter of a

running average is expressed as follows:

$$f(x, y) = \begin{cases} \dfrac{F_0}{\pi r_0} & : 0 \leq r \leq r_0 \\ 0 & : \quad r \geq r_0 \end{cases} \tag{2-4}$$

where, $r=\sqrt{x^2+y^2}$ and F_0: magnification. Fourier transform of this formula is given by,

$$F(\omega_1, \omega_1) = 2F_0 \frac{J_1(\omega r_0)}{\omega r_0} \tag{2-5}$$

where, $\omega=\sqrt{\omega_1^2+\omega_2^2}$ and J_1 is the first order of Bessel function.

Seya's filter is described by two filters of running averages as follows:

$$f(x, y) = \begin{cases} \dfrac{F_0}{\pi}\left(\dfrac{1}{r_0^2}-\dfrac{1}{r_1^2}\right) & : r_0 \leqq r \leqq r_1 \\ 0 & : r_1 < r < r_0 \end{cases} \tag{2-6}$$

Therefore, its characteristic function is given as follows:

$$F(\omega_1, \omega_2) = 2F_0\left(\frac{J_1(\omega r_0)}{\omega r_0}-\frac{J_1(\omega r_1)}{\omega r_1}\right) \tag{2-7}$$

The characteristic curves for r_1/r_0=2.0, 2.5 and 3.0 are shown in **Fig. 6.** We adopted r_0/r_1=3.0.

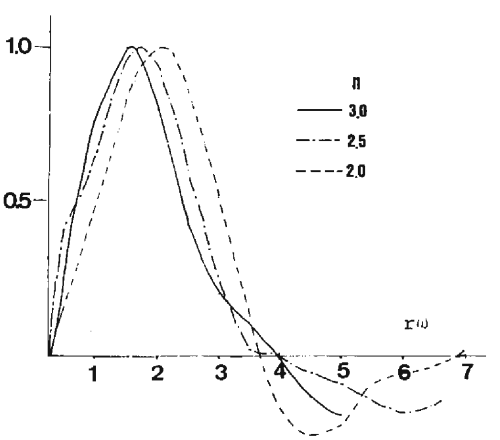

Fig. 6. Normalized characteristic curves of Seya's filters. Ratios of radii are 2.0, 2.5 and 3.0. Abscissa indicates $r_0\omega$.

(2) Analysis of a model

Seya's filter was applied to a short column as shown in **Fig. 7.** The band-pass

filter extracts the rim of the column. We adopted 1/3 as the ratio r_0/r_1. The pattern of the 3-dimensional running averages given by a moving circle is shown at the upper left and right in **Fig. 7** for the cases of the radii of 3 and 1, respectively. The result given by the band-pass filter is obtained by subtraction of the latter from the former as shown at the bottom in **Fig. 7.**

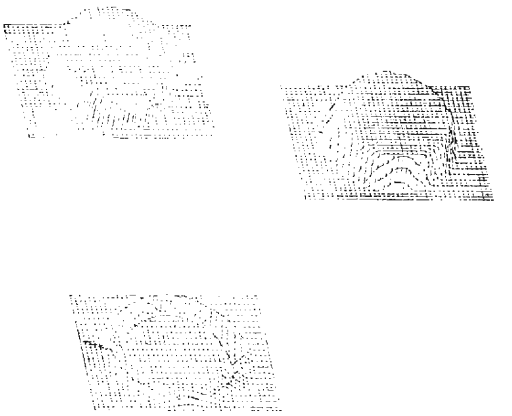

Fgi. 7 Results of application of the Seya's band-pass filter to a model which is a column with low height
Upper left: running average in a case of radius 1
Upper right: running average in a case of radius 3
Lower: the results obtained by subtraction of upper left from upper right

(3) Analysis of topography

A band-pass filter with a central wavelength of 40 km and a band width of 20–90 km was applied to topography for extracting long and intermediate wavelengths. For extracting short and intermediate wavelengths, a band-pass filter with a central wavelength of 20 km and a band width of from 10 to 40 km was used. The extracted topographies are shown in **Figs. 8-a, b** and **c**. In **Fig. 8-c**, the coast and contour lines are superimposed on **Fig. 8-a** for sake of easy understanding.

(a) Analysis of topography

Although the topography with long wavelengths was not distinctly identified in the results of the 2-dimensional Fourier analysis, it is clearly observed in **Fig. 8-a.** This topography is classified into two kinds by strike. One is an NS strike in which the long axis is nearly oriented the NS direction, and another is an EW strike.

Topogarphy with an NS strike.

Fig. 8-a shows that topography with long wavelength in the Chubu district between the ISL and TIL are represented by several large mountain ranges which extend over 200 km in a nearly NS direction. They are the Hida (No. 2 in **Fig. 2**), Kiso (No. 3) and Akaishi (No. 1) mountain ranges. In the western part of this district, there is also a long mountain range in the NS direction which extends from the Hokuriku to the northern Kii peninsula (see **Fig. 2**). It is to be noted that this

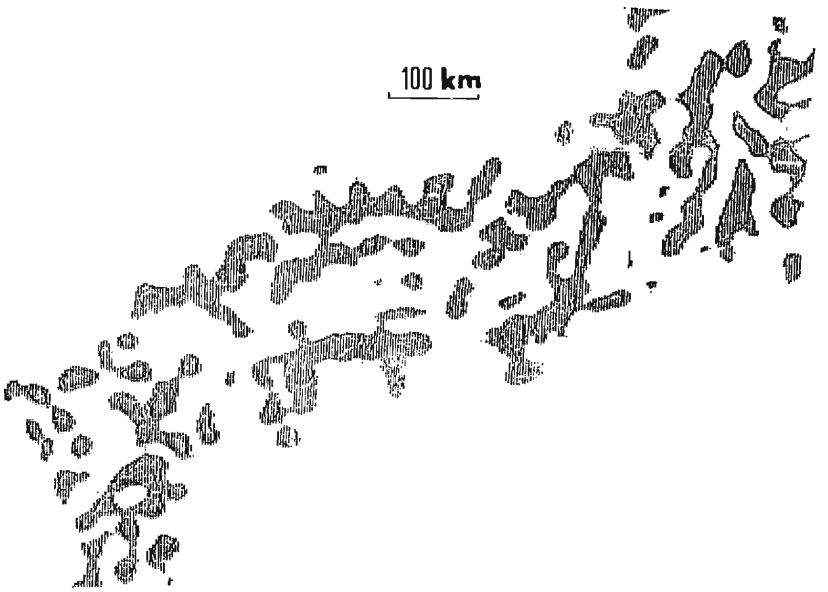

Fig. 8-a Pattern of topography extracted by a band-pass filter with a central wavelength of 40 km. Band width is between 20–90 km. Shadow part indicates positive area corresponding to upheaval region. White area indicates negative area.

mountain range is encountered and terminated by the MTL running in the EW direction.

Topography with an EW strike.

In the Chugoku and Shikoku districts, there appear topographies with long wavelengths extending in an EW direction. The Chugoku mountain range measures 200–250 km along the EW direction and its width is 50–70 km. The Setouchi peneplain (No. 6 in **Fig. 2**) is parallel to the Chugoku mountain range. The Shikoku and Kii mountain ranges are also parallel to the Chugoku mountain range. Thus, this region ocmposed of the Chugoku, Shikoku and Kii peninsula is characterized by a large, undulatory landform in the NS direction. The Kanmuri-yama mountains on the west side of the Go river (E in **Fig. 2**) has a different aspect from the Chugoku mountains.

(b) Topography with intermediate wavelengths

According to **Fig. 8-a** and **c**, the long mountain ranges such as the Hida, Kiso and Akaishi, described above seem to be made up of a continuation of some smaller mountain blocks about 50 km long. The same aspect may be seen as well in the case of a long mountain range extending from the Hokuriku to the Kii peninsula.

It can be recognized in **Fig. 8-a** that the Chugoku mountain range consists of several smaller mountain ranges, 50–100 km long in the NS direction perpendicular to the Chugoku mountain range. This structure is interesting and will be treated later in chapter 4. In the Outer Zone, especially in the Kii peninsula and Shikoku,

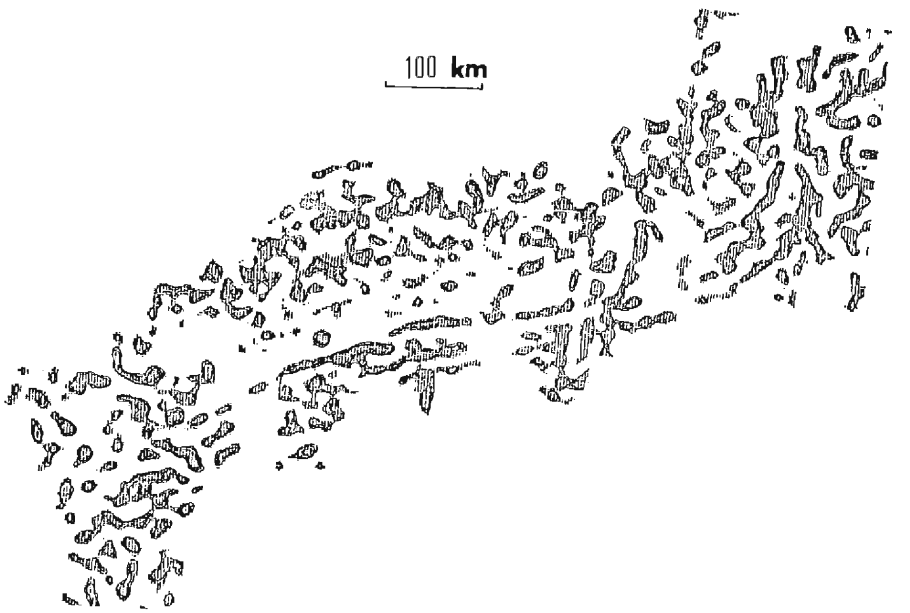

Fig. 8-b Pattern of topography extracted by a band-pass filter with a central wavelength of 20 km. Band width is between 10–40 km. Shadow and white parts have the same meanings as Fig. 8-a.

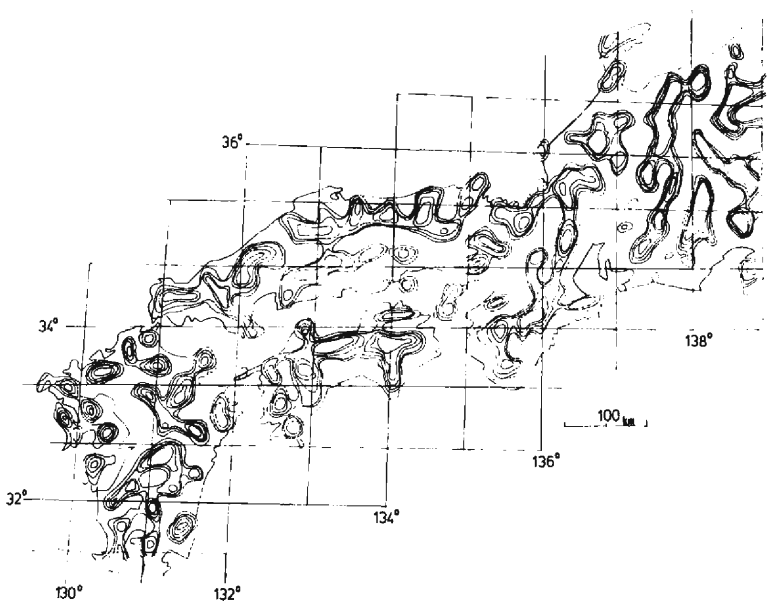

Fig. 8-c Coast and contours are superimposed on Fig. 8-a.

there are clear intermediate mountain ranges both in the NS and EW directions, referring to **Fig. 8-a** and **b**.

(c) Topography with short wavelengths

Comparing **Fig. 8-b** of short wavelengths with **Fig. 8-a** of long ones, it is remarkable that topography with the short wavelength shows much larger regionality than that with the long wavelength. Topography with the short wavelengths in the Chugoku district is very irregular, while those in the Outer Zone and Chubu district are rather rgeular. In **Fig. 8-b**, narrow and relatively long mountain ranges both in the EW and NS directions are seen in the Outer Zone of Shikoku and the Kii peninsula. Also in the Chubu district, narrow mountain ranges trending approximately in the NS direction are observable up to the Hokuriku-Kii peninsula line which is the west boundary of this district.

In the northern Kinki and Chugoku districts, topographies of the short wavelengths are complicated, and no regularity is observable. This character of the short wavelength in these two districts will be re-considered in chapter 4.

3. Topography with long wavelengths and folds

As already mentioned in the Introduction, some geomorphologists and geologists have conjectured that undulations of topography in many cases were formed by folding. In the foregoing two chapters, topographies corresponding to various wavelengths had been produced, and these made it more persuasive to consider the formation mechanism of the undulatory topography by folding. In this chapter, we shall briefly describe the fold theories and experiments so far presented and then try to provide some interpretations on undulatory topographies, mainly of long wavelengths from the viewpoint of folding.

3.1. Experiments and theories of the folding

The studies on geological folds began in the 19th century. Wills[23] took an interest in the fold in the Appalachian mountains, and suggested buckle folding as a mechanism of the fold on the basis of experiments. In the present century Smoluchowski[24),25] established the basis of study of fold. He revealed that the elastic constants were determined by the ratio between the wavelength and thickness of the folding layer using a buckling model of an elastic body. Biot[26] attempted to do the same kind of experiment by using a visco-elastic body. He also indicated that the fold was born from buckle instability of visco-elastic body, and proposed the following formula:[27]

$$Ld/h = 2\pi \sqrt[3]{\eta/6\eta_1} \tag{3-1}$$

where, Ld is dominant wavelength, h is the thickness of folding layer, η is a viscosity coefficient of folding layer and η_1 is a viscosity coefficient of the embedded body.

The same formula was derived by Ramberg[28] from studies of fluid mechanics.

Biot's formula is applicable under the conditions that the ratio Ld/h be greater than 10 and also the viscosity ratio $1/n$ be greater than 100. But observations by Sherwin and Chapple[29] gave smaller values of the ratio of Ld and h. They improved the formula by introducing a concept of buckle shortening and proposed a formula as follows:

$$Ld/h = 2\pi \sqrt[3]{(S+1)/12nS^2} \tag{3-2}$$

where, Ld: wavelength

S: final value of quadratic elongation

$S=(1+\varepsilon)^{-2}$

$\varepsilon=(Ld-L_0)/L_0$

$n=\eta/\eta_1$: viscosity ratio

L_0: original wavelength.

This formula indicates that the ratio, Ld/h, decreases along with the development of fold. It means increase of S.

3.2. Topography with long wavelengths as a result of folding

One of the typical topographies of long wavelengths' in Southwest Japan is, as shown in **Fig. 8-a** that of wavelengths of 50–150 km with an EW strike. This is, referring to **Fig. 2**, composed of the Chugoku mountains, Setouchi peneplain and Shikoku mountains. The second is that of nearly the same wavelengths 50–70 km with an NS strike in the Chubu district, composed of the Hida, Kiso and Akaishi mountains and a mountain chain extending in the NS direction from the Hokuriku district to the eastern Kii peninsula.

These two large topographies of EW and NS strikes are considered to be the fold topographies formed by compressive stress in the NS and EW directions, respectively, as asserted by many researchers so far. If we assume the wavelength, which corresponds to the distance between the Chugoku and Shikoku mountain ranges, is 150 km, and the thickness of folding layer, probably which corresponds to the crust, is 30 km, the viscosity ratio in Biot's formula (3–1) would be obtained as $1/n=3$. This value is too small to apply the Biot's formula. If instead we assume the existence of shortening proposed by Sherwin and Chapple[29], a smaller value for the viscosity ratio is reasonable. For example, when $Ld=150$ km and $h=30$ km are given the viscosity ratio obtained is about 2–40, and the shortening is about $S=2$–8. If $S=2$, $1/n$ becomes 4 and the shortening is 30%. The increase of the folding amplitude is estimated to be slightly less than 1 km[30]. In the case of the Chubu area, when $Ld=70$ km and $h=30$ km are assumed, 1/n is obtained as 2–16. Increasing of the amplitude is not greater than about 500 m. If we assume 1,000 m as the present average elevation, and if an uplift is assumed as about 500 m, it would take 500,000 years to complete the uplift, as the mean velocity of vertical deformations is 1 mm/yr estimated from various investigations.[31),32),33)] This value, 500,000 years, does not seem entirely erroneous as the period of deformation in Southwest Japan. Threefore,

the idea that these large mountains have been formed by folding is not unreasonable. Two tectonic compressions in the NS and EW directions are considered to be produced by the subduction of the Philippine Sea plate and Pacific plate, respectivdely. In **Fig. 8-a**, the topography of an NS strike with long wavelengths changes its strike, as mentioned above, at the mountain chain extending in the NS direction from the Hokuriku district to the eastern Kii peninsula. To the west of this mountain chain, the strike of long wavelength topography is oriented into the NE-SW direction in the northern Kinki district, and then changes into the EW direction in the Chugoku district. Namely, in the northern Kinki district, there exists some interactions of both effects by the Pacific plate and the Philippine Sea plate. We can see that the long mountain chain from the Hokuriku region to the Kii peninsula intersects the Kii mountains with the EW strike at southern Kii peninsula. This fact is also an evidence of interaction of the two different compressive stresses in this district.

Thus, the framework of topography in Southwest Japan is constructed of two topographies of long wavelength which are arranged systematically in the EW and NS directions.

3.3. Discussions

The Pacific plate subducts in N70°–80°W direction and with a dip of 20°–40°[34] in Northeast Japan. The compressional stress with nearly EW direction derived from this subduction affects over all the Tohoku region.

According to Huzita (1980)[35], the effects of this EW compressional stress reach to the Chubu district through the Fossa Magna. This is proved by the existence of dip-slip fault with NS strike like the Atera fault. The NS alignment of volcanoes, and dikes with EW strike[36].

On the other hand, according to investigation on the mechanisms of great earthquakes occuring along the Nankai torugh[37], the Philippine Sea plate subducts in N20°–45°W direction and with a dip of 20°–25°, and with velocity of 3–4 cm/yr[38] in Southwest Japan.

Since the subduction of the Pacific plate is of a large scale, extending down to a depth about 700 km, it is understandable that the topography of NS strike with long wavelengths has been formed by the compressional stress of the Pacific plate, as mentioned above.

However, the circumstances are somewhat problematical regarding the Philippine Sea plate. The present depth of the leading edge of this plate is considered to be 80 km at most from various points of view, for instance, depth distribution of earthquakes relating to the subduction of this plate[39),40] and the uppermost mantle structure obtained from various types of seismic waves[41),47] such as reflected waves, refracted waves and transformed waves at the plate boundary. However, the subduction of the Philippine Sea plate appears to have reached to a much deeper place in older geological times, considering the facts that volcanoes of the Quaternary distributed along the northern coast of the Chugoku district are composed of high alkaline basaltic rocks which are considered to have derived from the deeper mantle[43] and that

there seems to exist some parts with high seismic velocity at depths of 100–150 km below the Chugoku mountains[44], which are supposed to be some fragments of the plate in much older times. There still remains a question which of the two plates has formed the large topography of an EW strike in the Chugoku and Shikoku regions, the present plate with shallow subduction or the presumed old plate with much deeper subduction. In any case, the prevalence of NS compression in these districts in much older geological times is supported by the facts that the Yamasaki fault (see **Fig. 19**) was of right lateral strike-slip before the Quaternary period[45], in spite of left lateral movement at present, and that veins in the Miocene are arranged in a direction suggesting NS compression at that time[46].

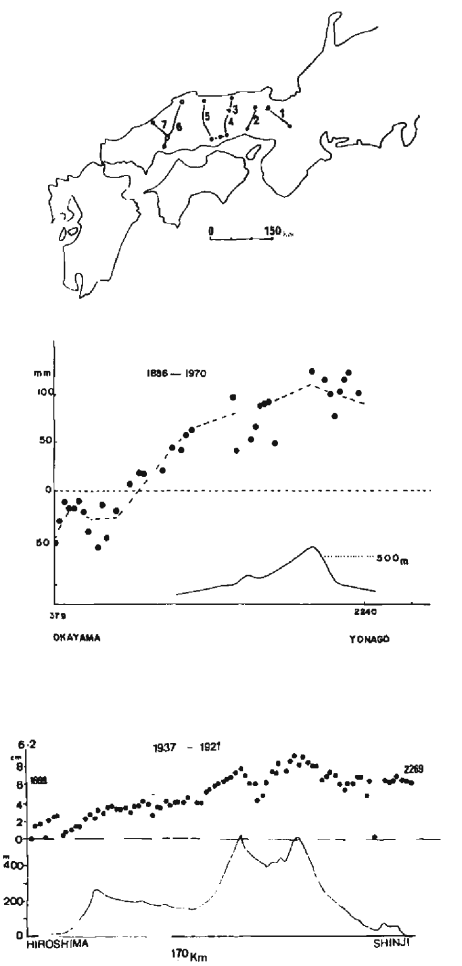

Fig. 9. Routes and results of leveling surveys across the Chugoku mountains
Upperr: the routes of leveling surveys
Middle: result of leveling survey and topography along route No. 5
Lower: result of leveling survey and toppography along route No. 6

Next we shall consider the results of geodetic surveys in order to examine the present crustal movement. **Figs. 9** show routes and results of leveling surveys in the Chugoku district which have been carried out since the end of the 19th century[47]. In **Figs. 9-b** and **c**, solid lines and dots represent the topography along the route and values of level change, respectively. In both figures, uplift is advancing in parallel with the topography, and its velocity amounts to 1 mm/yr or more. This deformation velocity is of the same order as that of the mean velocity throughout recent geological time[31),32),33)]. On the other hand, the results of triangular surveys[48)] show that a horizontal compression in an NS direction is now acting on the area concerned. These results of geodetic surveys tell us that the present Philippine Sea plate still has enough energy to cause the deformation of topography in the Chugoku district.

According to the results of seismic observations, on the other hand, almost all earthquakes in the upper crust in the Chugoku and Shikoku districts show that these have been generated under horizontal compresskion in the EW direction. It is a question why earthquakes showing NS compression do not ocucr there, if the energy of the Philippine Sea plate is sufficiently large as shown above. Ichikawa[49)] stated that earthquake generating compressive stress in the Shikoku district changed its direction from NS to EW during 1944–1946 when two great earthquakes, the 1944 Tonankai and 1946 Nankaido earthquakes, occurred. This suggests that the Shikoku district is a place of competition of two tectonic compressions.

It is difficult at the present stage to discuss whether or not there is any difference between statioanry stress yielding topographical deformations and the dynamical stress generating earthquakes.

4. Topographies with short and intermediate wavelengths and crustal block

4.1. Fold topography with short wavelengths

We have earlier said in 2.3, (3), that topographies with short and intermediate wavelengths are complicated, as shown in **Fig. 8-b**, compared with that of the long wavelength, and also regional differences are larger in the former. In this chaper, some features of topographies with short and intermediate wavelengths together with formation mechanisms will be investigated.

In Fig. 8-b which was extracted by a band-pass filter with a central wavelength of 20 km and a band width from 10 to 40 km, one of systematic alginments of topography is "NS stripes" defined in 2.2, (3) which have a wavelength of 30–50 km and distributed in the Outer Zone and the Chubu district. The pattern of alignments of this topography in the Chubu district is the same as that with long wavelengths and NS strike as mentioned in the previous chapter. Moreover, this topography with short wavelengths exists from the ISL to the mountain chain from the Hokuriku district to the Kii peninsula, but not in the western area of this

mountain chain. This fact also the same as in the case of long wavelength topography. Judgign from these investigations, the topographies with short wavelengths in the Chubu district and in the Outer Zone as well seem to have been formed in the same way by EW compression from the Pacifici plate.

On the other hand, there are "EW stripes" in the south side of the MTL in the Kii peninsula, which are parallel to the MTL and intersect with NS stripes there. These EW stripes are considered to be due to NS compression from the Philippine Sea plate. Moreover, these NS and EW stripes should be foldings of the upper crust from the viewpoint of shortness (30–50 km) of the wavelength. In fact, these short wavelength topographies may have the thickness of the folding layer such as 8–10 km, in view of the result of Sherwin and Chapple[29].

The topography with the short wavelengths shows strong locality, differing from the regularity in the arrangements of topography with long wavelengths. We can not recognize, in **Fig. 8-b**, any systematic topographies in the Chugoku and the northern Kinki districts. It is to be noted that the pattern of alignment of topography differs between the Chugoku district in the Inner Zone and the Shikoku district and the Kii peninsula in the Outer Zone. This fact may be related either to the features and history of the Philippine Sea plate as discussed in 3.3, or to properties of rocks composing the upper crust in the districts concerned. Because, according to Okuda, the amount of erosion is smaller than the altitude derived from uplift of the crust. His observation in Southwest Japan gives about 3/1,000 mm/yr[50] as the amount of erosion.

4.2. Topographies with intermediate wavelengths in the Chugoku and northern Kinki districts

Topography with short wavelengths shown in **Fig. 8-b** is very complicated in the Chugoku and the northern Kinki districts west of Lake Biwa, and it is difficult to say that any regularity are clearly recognized in the figure. **Fig. 10** is topographies

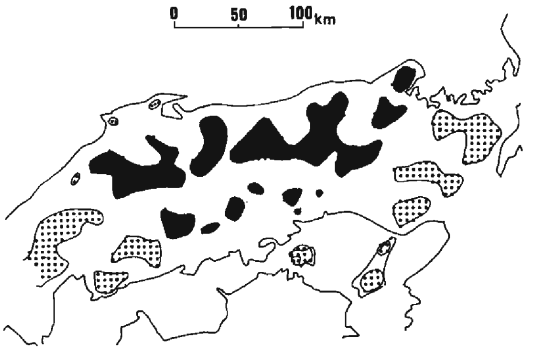

Fig. 10. Pattern of topography extracted by a band-pass filter with a central wavelength of 30 km. Band width of the filter between 25 and 65 km. Dark area indicates the Chugoku mountains and Setouchi peneplain.

mainly in the Chugoku district, which was extracted by a band-pass filter with a central wavelength of 30 km and with a band width of 25–65 km. Black parts indicate uplifts, which have the dimension of about 50 km and nearly an NS strike and are aligned in the EW direction along the Chugoku mountain range and the Setouchi peneplain. As shown in **Fig. 8-a**, the Chugoku mountain range and the Setouchi peneplain are the topography with long wavelengths, 50–150 km, and an EW strike. The results shown in **Fig. 10**, therefore, indicate that the Chugoku mountain range and the Setouchi peneplain suffer a double folding. Namely, one is fundamental folding with long wavelengths and an EW strike and another is of the intermediate wavelengths and an NS strike superposing on the former. **Fig. 11** is a schematic explanation of this double folding. We must, therefore, consider that the Chugoku district had suffered EW compression from the Pacific plate as well as NS compression from the Philippine Sea plate. These topographies with intermediate wavelengths and an NS strike are also recognizable in Fig. 8-a showing the topographies with long wavelengths.

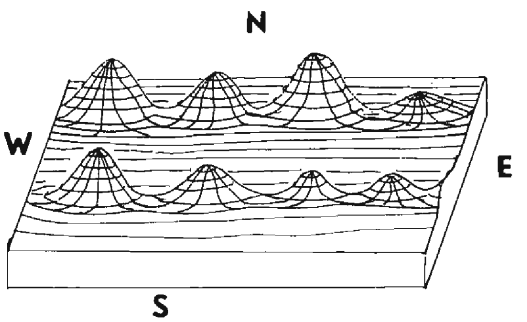

Fig. 11 Schematic representation of the Chugoku area, which has suffered double folding by NS and EW compressions. The northern and southern mountains indicate the Chugoku mountains and hills in the Setouchi peneplain, respectively.

Topography with intermediate wavelengths in the northern Kinki district shows the same complexity and irregularity as those with long and short wavelengths. Those facts may suggest that the above two compressions are in competition with each other for all wavelengths.

The topography of the Kanmuriyama mountains on the west of the Go river (E in **Fig. 2**) is different from that of the Chugoku mountains and rather similar to that in the Kyushu mountains. This problem, however, should be discussed after observational data in geophysics including seismology will be accumulated in future.

4.3. Partition of the crust into blocks and the role of rivers

Most rivers in the Chugoku district between the YKL and the Go river flow northward or southward straight without meanders, as shown in **Fig. 12**. **Fig. 13**[51] is a composite figure of the topography with intermediate wavelengths (**Fig. 10**) and

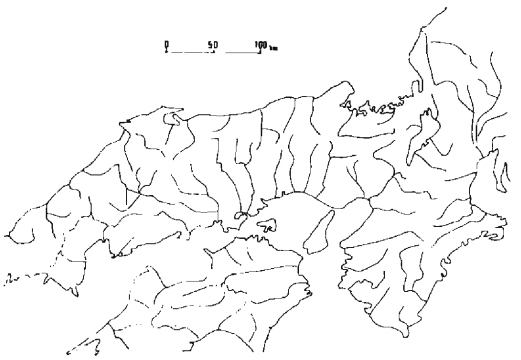

Fig. 12 Distribution of main rivers in the Chugoku and other districts

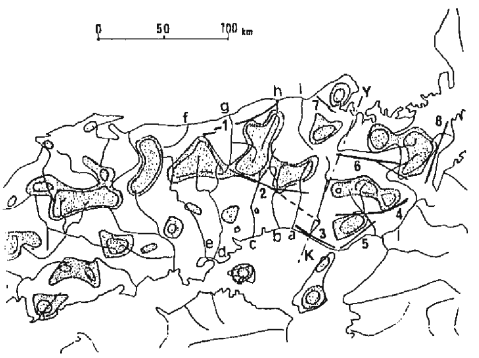

Fig. 13 Map of extracted topography, rivers and active faults
Numerals and letters indicate active faults and rivers,

1 : Yoshioka-Shikano faults,	2 : Yamasaki fault,
3 : Takasago tectonic line,	4 : ATL (Arima-Takatsuki Tectonic Line),
5 : Suma-Suwayama fault,	6 : Mitoke fault,
7 : Go-mura fault,	8 : Hanaore fault,
a : Ichi river,	b : Ibo river,
c : Chigusa river,	d : Yoshii river,
e : Asahi river,	f : Tenjin river,
g : Sendai river,	h : Yata river,
i : Maruyama river,	Y–K : YKL.

distribution of rivers (**Fig. 12**). As shown in **Fig. 13**, most uplift parts of folding are located between two rivers. This phenomena may be natural, considering that the area between two uplift parts is a subsidence part made by folding. It is to be noted, however, that the crust in this district appears to be composed of many rectangular blocks long in the NS direction and arranged systematically in both the EW and NS directions as seen in **Fig. 13**. This may indicate that the crust in this district originally suffered double foldings by two compressions in the EW and NS directions shown in **Fig. 11**, which facilitated such a systematic partition of the crust as stated above.

Partitioning the crust in the northern Kinki district has been done in a complicated manner, and regular arrangement of rectangular blocks is not seen. But the uplift parts of topography is surrounded by rivers and also by geological faults which prevail particularly in this area, resulting in many crustal blocks.

Many rivers are considered to have been formed by tectonical causes, as mentioned above, such as subsidence parts of folding, the trace of the faults on the surface, and so on. This presumption is supported, as will be shown in chapter 6, by the fact that many microearthquakes occur along the river bordering two blocks.

Such a partition of the crust into blocks is clearly seen in the Chugoku and the northern Kinki districts, and not in other districts, for instance, in the Shikoku and Chubu districts. This phenomena may be due to differences in tectonic conditions and properties of the crustal rocks.

5. Crushed zone as a boundary of the crustal blocks

As already mentioned in 4.3, it appears that partition of, probably, the upper crust into small blocks has developed in the Chugoku and the northern Kinki districts. In the northern Kinki district, in particular, faults tend to become boundaries between the blocks as in many cases. In this chapter, we shall adopt the Yamasaki fault as an example of such faults and investigate its features.

The Yamasaki fault is situated in Hyogo Prefecture in the northern Kinki district. It is one of the largest active faults in the Inner Zone, of left lateral strike-slip, and 80 km long in a WNW-ESE direction. This fault has been investigated since 1975 by various observations as a test-field for earthquake prediction.[52),53)54),55),56),57)58)]

5.1. Microearthquake activity and crushed zone

As we shall discuss in detail in chapter 6 regarding the relationship between earthquake occurrence and active faults, we shall adopt here only one seismological phenomenon which seems to be related to topography and crushed zone.

Epicenters of microearthquakes are distributed not just on the trace of the Yamasaki fault on the ground surface but on the north side of the trace as a belt severla kilometers wide along the fault. We calculated the density of earthquake occurrence, namely the numbers of microearthquakes in a unit area which is the same as that used in chapter 2. The microearthquakes used here are those observed by the Tottori Microearthquake Observatory, Disaster Prevention Research Institute, Kyoto University during the period from January, 1970 to June, 1978. **Fig. 14** is a superposed representation of topography, tectonic lines and the density of microearthquake occurrence. In the figure, A denotes the Yamasaki fault system, in which a dotted line is called Kuresakatoge fault. A contour of topography represents 600 m and hatched parts denote mountain areas higher than 600 m. The density of microearthquake occurrence is shown by three ranks, 10 or more, 5 to 9 and 3 to 4. A straight line B was drawn in the following manner: We can see that

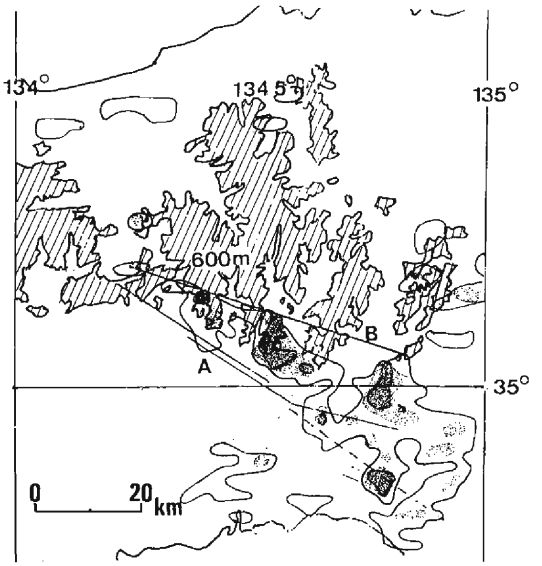

Fig. 14 Distribution of density of microearthquake occurrences and topography. Contours indicate 600 m height and hatched area is higher than 600 m. Dark shadow indicates density 10 or more times, pale one between 9 and 5, and inside of contour 3 or more.
A: the Yamasaki fault system
B: a straight line through the presumed kern-cols

several small mountainous blocks are connected to the south margin of large mountainous area higher than 600 m by narrow and limited part. Therefore, this topography seems to represent kern-but (small mountainous block), kern-col (limited part) and tectonic line (B). As seen in **Fig. 14**, microearthquake activity is high between the Yamasaki fault system and a supposed tectonic line B. This fact may suggest that crushing of crustal rocks has developed between lines A and B, and it brings about high activity of microearthquakes. Accordingly, the Yamasaki fault system seems to be from the viewpoint of earthquake generation, not a sharp boundary but a crushed zone with rather wide width of, say, 10 km or more.

5.2. Surveys of underground water and electrical resistivity measurements

Observations of ground water, regarding its level and other factors such as its temperature or chemical components, were carried out using wells which are distributed across the Yamasaki fault as shown in **Fig. 15**.

Fig. 16 shows, in order from the top, the elevation of the well, the depth of water level measured from the ground surface and the height of water surface from sea level (water head). Abscissa in the figure denotes the distance in km of the well measured from the center of the fault, which is the most conspicuous left lateral offset line of this fault from the viewpoint of geology.

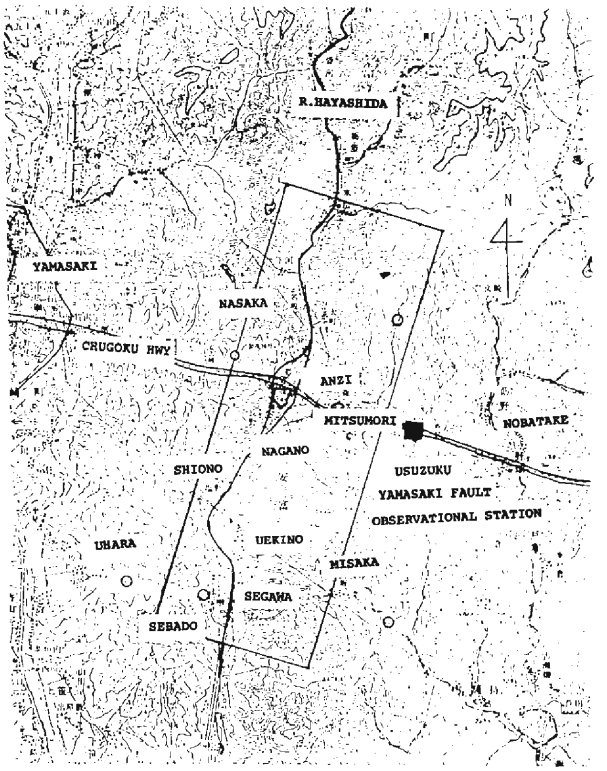

Fig. 15 The region in which observation of ground water was carried out. Wells in the rectangular area were used. The Yamasaki fault nearly corresponds to the Chugoku Highway.

Elevation of the well is higher on the north side, and becomes lower gradually to the south. The gradient is steeper near the fault. The water level decreases suddenly from north to south at the fault trace, and then increases gradually. At $x=-2$ km, the route of the survey intersects the Kuresakatoge fault and at that point the depth of the water surface begins to decrease. Between $x=-2$ km and -3 km, the depth of the water surface shows a triangular distribution pointed downward. On the other hand, the water head distribution has a peak on the north side of the Yamasaki fault.

These phenomena regarding well elevation, water level, and water head suggest that southward flow of the ground water is dammed up on north side of the fault by fault clay existing near $x=0$. Since there was no well in the zone between the two faults, we could not know the exact aspect of ground water there. In this area, however, there are some reservoirs of city water and there are no drought of ground water in any season and no change of ground water at the time of rain fall, and moreover we can see many self-gushing springs there. From these facts, this zone is considered to be full of ground water, which may suggest that this zone is

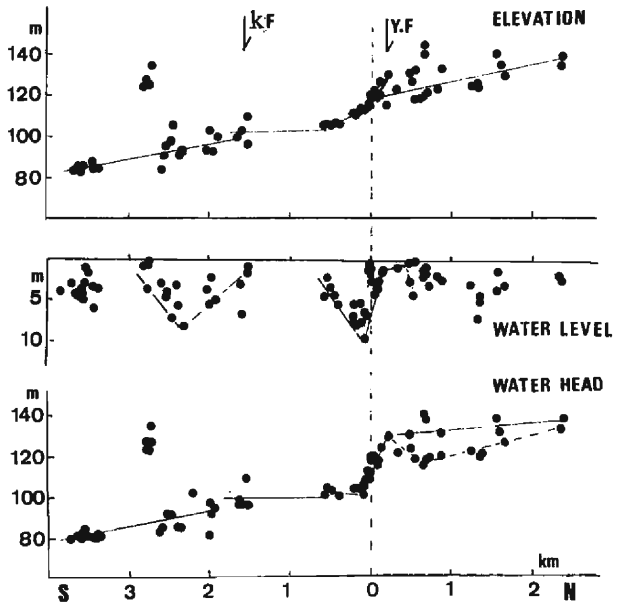

Fig. 16 Results of ground water survey
Upper: elevation of place of wells
K.F. and Y.F. indicate the Kuresakatoge and Yamasaki faults inferred from this survey, respectively
Middle: water level distribution
Lower: water head distribution

very porous, namely a crushed zone. From these results as for ground water, we can suppose a crushed zone with a width of 3–4 km including both the Yamasaki and Kuresakatoge faults.

An electrical resistivity survey was carried out at the Yamasaki fault by Handa and Sumitomo[54]. This method gives a distribution of electrical resistivity of underground rocks, using electromagnetic waves of ELF band. According to the survey's result shown in **Fig. 17**, the area of low resistivity was found mainly on the north side of the Yamasaki fault with a width of 4–5 km and with the depth range down to 1 km or more.

5.3. Discussions

We have examined the features of the Yamasaki fault as a boundary of crustal blocks on the basis of microearthquake activity, ground water and electromagnetic resistivity of the underground rocks. These observations point out that the Yamasaki fault system is not a group of sharp surfaces but a crushed zone with some width. The location and width of the crushed zone, however, differ depending upon the kinds of observations. Those inferred from microearthquake activity have the widest spread of 10 km or more to the north.

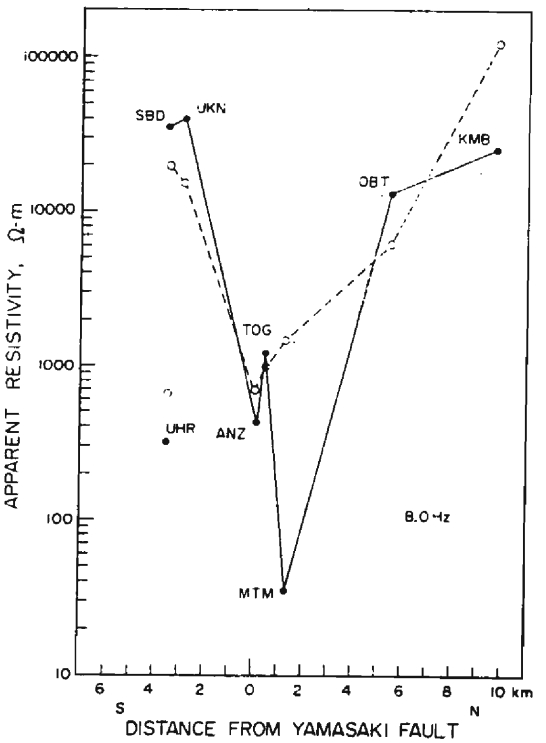

Fig. 17 North-south profile of apparent resistivity across the fault from measurements of 8 Hz variations in the electric and the magnetic field. Solid circles indicate the apparent resistivities obtained from the ratios of the electric field components normal to the fault strike to the magnetic components parallel to that. Open circles are from the electric components parallell to the fault strike to the magnetic components normal to the fault (after Handa and Sumitomo, 1979).

On the other hand, observations of underground water and electromagnetic resistivity of rocks show the existance of a crushed zone of different aspects than described above.

6. Topography and earthquake occurrence

6.1. Relation between large earthquakes and topography

The following catalogues for large earthquakes were used: 1) Damaging earthquakes in Japan published by Usami[59], 2) Annual table of natural sicence[60] ("Rika Nenpyo" in Japanese), 3) Catalogue of moajor earthquakes which occurred in and near Japan (1926–1956) by JMA[61]. The data compiled by Utsu[62] were also referred to. The earthquakes used have been restricted to those later than 1850, because of their accuracy.

Most of the earthquakes occur in the upper crust down to a depths of 15–20 km. Moreover, tectonic deformations in the crust over long time range seems to reflect the topography of short wavelengths. From these reasons, we adopted the topography extracted by the band-pass filter with a central wavelength of 20 km, as a reference topography in order to investigate the relation between the large earthquakes and topography. In **Fig. 18**, epicenters of the large earthquakes and active faults are plotted on thus extracted topography. It may be noticed by close examinations that most earthquakes and also active faults appear to be distributed along the margins of the uplift parts.

One possible mechanism of formation of the faults is indicated by the folding theory as follow: namely, along with the development of the fold, shearing stress concentrates at limbs of the fold[63], the strength of rocks there decreases[64], and even small increase of the stress brings about fracture of the rocks. The fault with such a mechanism of formation is of dip-slip type. The fault of this kind will be continuously predominant, if the tectonic compression continues to act normally to the fault strike as in Northeast Japan. However, if direction of compressional stress changes after formation of the dip-slip faults, these existing faults can give rise to strike-slip movement uner some conditions. According to Mckenzie[65], a preexisting fault can occur failure by acting of the greatest principal stress in a limit of

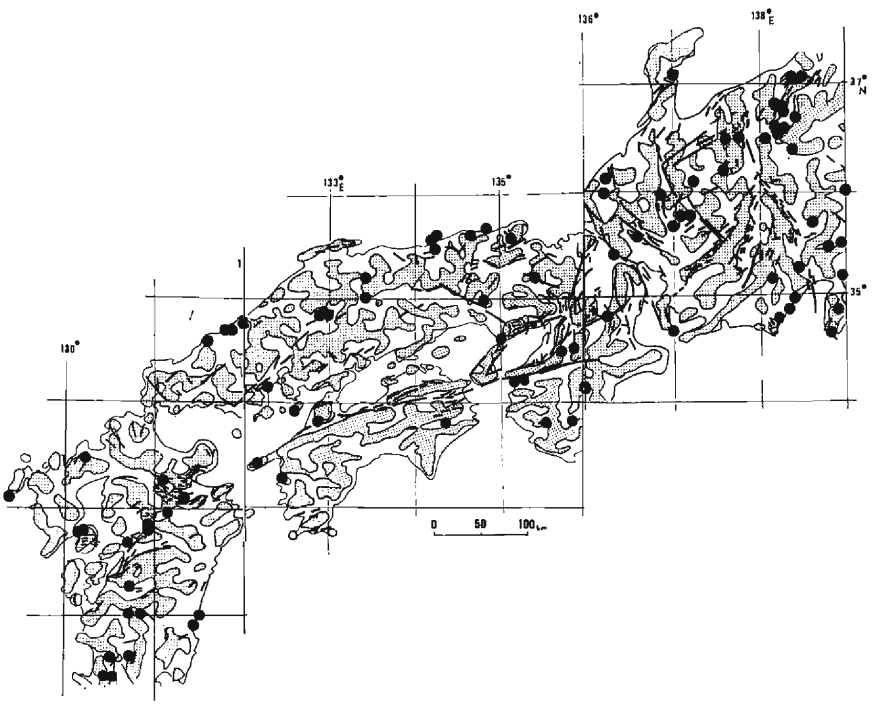

Fig. 18. Main active faults and large earthquakes which occurred during 1850 to 1975 are superimposed on the topography extracted by band-pass filter with a central wavelength of 20 km

orientation determined by the values of principal stresses.

The topography with long wavelengths and EW strike composed of the Chugoku and Shikoku mountain ranges seems to have been formed by NS compression of the Philippine Sea plate as described earlier, and then the MTL, perhaps the Yamasaki fault and others were produced as a dip-slip fault in the above manner. These dip-slip faults are considered to have begun to exhibit the strike-slip movements, since the compressional stress in these districts changed its direction from NS to EW. Huzita (1968)[66] investigated the tectonical structure in and around the Rokko mountain area. He stated from the observations that tectonic stress pattern changed from NS compression to EW one at the middle of the Quaternary in Southwest Japan. The fault system in the Rokko mountains was composed of reverse fault with an EW strike in the Plio-Pleistocene but after the middle of the Pleisticene the fault system had changed the strike into the NS direction and movement of the old faults with an EW strike began to be dominant in lateral direction. And he also mentioned that such a reverse fault system with an NS strike makes mountainous topography with axes of the NS direction. Sangawa (1977)[67] investigated tectonics in the Kii peninsula. His results have reached to the same conclusions derived by Huzita (1968)[66] as follows: the MTL had moved in the Plio-Pleistocene as a reverse fault which was found in the lower sediment along the MTL in the middle Kii peninsula, and then the uplift movement becoming weak, the right lateral movement began to be dominant after the middle of the Pleistocene; such lateral movement is found in the upper sediment along the MTL in the mountainous region. These facts indicate that the stress pattern changed in the same manner and at the same time as mentioned by Huzita (1968)[66].

6.2. Relation between microearthquake occurrences and topographies of long and short wavelengths

Routine observations of microearthquakes were commenced around 1965 as a part of the "Earthquake Prediction Research Project in Japan". In the northern Kinki district, observation of microearthquakes has been continued since 1965 by the Tottori Microearthquake Observatory and the Abuyama Seismological Observatory, Kyoto University. Telemetering observation was commenced during 1975–1976 at the two observatories[68),69)], and has brought about much higher accuracy in the observations.

Fig. 19 shows epicenter distribution of microearthquakes from Januray, 1970 to June, 1978 determined at the two Observatories. Dots, solid lines and broken lines in the figure indicate epicenters, active faults and supposed faults, respectively. The fact that microearthquakes are concentrated in a belt zone along a active fault was recognized at the Yamasaki fault soon after the commencement of microearthquake observations. One of the most obvious example of such a lineation is that observed along the Atotsugawa fault[70]. Another type of distribution is observed in which microearthquakes are distributed in groups. For example, a group of microearthquakes with about 30 km width observed on the north side of the Arima-Takatsuki

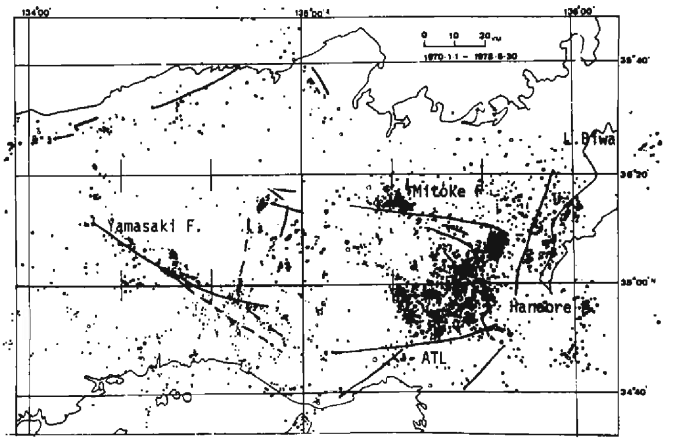

Fig. 19 Spatial distribution of epicenters of microearthquakes observed during the period from January, 1970 to June, 1978 by the Tottori Microearthquake Observatory and the Abuyama Seismological Observatory, Kyoto University. Solid lines indicate main active faults.

Tectonic Line (hereafter called ATL as shown in **Fig. 19**). These two types of distributions of microearthquakes come from the facts that in some cases, microearth quakes correspond to very small and sharp structures owing to their small source dimensions, and that in other cases, they correspond to a great many cracks distributed throughout the whole block owing to their large number of occurrences. Accordingly, to examine relations between both topographies of short and long wavelengths is needed, in order to investigate the possible relation between the microearthquake and the topography.

(1) Correlations to the topography with long wavelengths

Fig. 20 shows a composite graph in which the topography extracted by the band-pass filter with a central wavelength of 40 km and the epicenter distribution of microearthquakes are superposed. We can see nearly linear distributions such as those of the Yamasaki and the Yoshioka-Shikano faults. However, there are some other type of distributions. For instance, epicenters are located along the edges of a mountain block (A) on the north side of the Yamasaki fault or the Rokko mountains (B). Also, epicenters are distributed on the col between two mountain masses, like (C), (D) and (E) in the figure. These distributions (A) to (E), indicate that many microearthquakes occur on the boundary between the uplift and subsidence parts of the fold topography. These distributions seem to point out the existence of a fault at the limb of folding mentioned in the previous section, 6.1.

The most massive distribution may be a mass of microearthquakes on the north side of the ATL, as already mentioned above in this section. However, this group will be investigated in a later section, 6.2, (4).

Thus, we can say that distribution of microearthquakes indicates the present

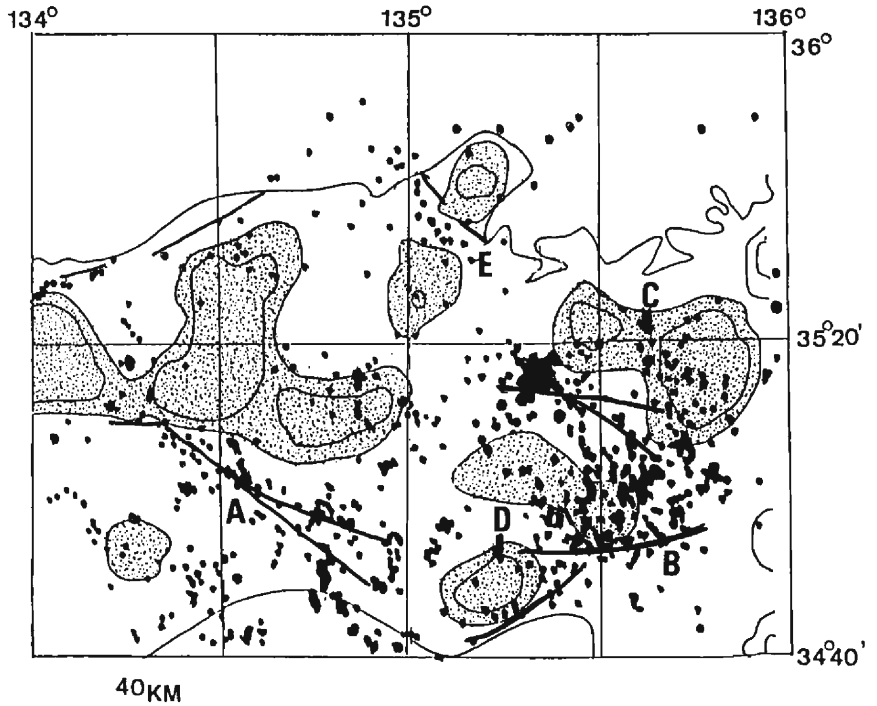

Fig. 20 Microearthquakes and active faults are superimposed on the topography extracted by a band-pass filter with a central wavelength of 40 km.
A, B, C, D and E indicate Yamasaki fault, ATL, Tamba and Rokko mountains and Go-mura fault, respectively.

state of the tectonic stress which has continuously devleoped the topography over long geological time.

(2) Correlations to the topography with short wavelengths

Fig. 21 shows epicenter distribution of microearthquakes superposed on the topography extracted by the band-pass filter with a central wavelength of 16 km. Microearthquake occurrences along the edges of large mountain blocks mentioned in the previous section (1) appear to be divided into distributions surrounding smaller mountain blocks, for example, a small mountain block (A) which is one part of the large mountain block, the Tamba mountains (B) and uplift part between the Yamasaki and Kuresakatoge faults (C). These examples which show microearthquakes correspond to very small topographies indictae that those topographies have tectonic significance.

(3) Contour lines of 300 and 600 m, and microearthquake distribution

In order to examine the topography with dimensions smaller than that treated in the above section (2), we shall consider landform itself. **Fig. 22** shows landforms with elevation with 300 and 600 m contours superposed by the epicenters of microearthquakes. As seen in the figure, many epicenters are located along the contours

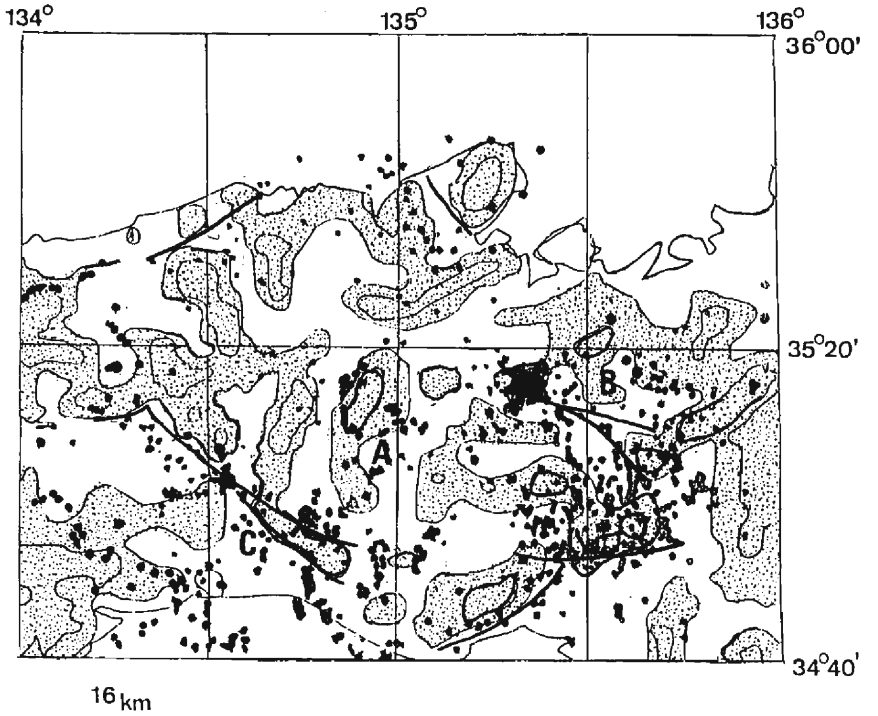

Fig. 21 Microearthquakes and active faults are superimposed on the topography extracted by a band-pass filter with a central wavelength of 16 km. Its band width is between 8 and 36 km. A, B and C indicate a small mountain, Tamba mountains and uplift part between the Yamasaki and Kuresakatoge faults.

as coming from with the mountain block, corresponding to the valley. This means that correlations of microearthquakes with the topography with short wavelength can be extended to still finer landforms. Also, this correlation indicates that even small ruggedness of topography, if relating to microearthquake occurrence, is not a superficial phenomenon but a manifestation of tectonics, because the depths of microearthquakes range from several to 20 km in this area.

(4) Distribution of microearthquakes relating to the Arima-Takatsuki Tectonic Line (ATL), and role of rivers

A massive distribution of microearthquakes on the north side of the ATL has dimensions of 30 km × 40 km. Its south edge is sharply bordered by the ATL, and there is almost no seismicity on the south side of it. We examine fine structures of this mass of microearthquakes. Numbers of microearthquakes (January, 1970-June 1978) per unit area, which have been described in chapter 5, are shown in **Fig. 23** by three different symbols depending on their numbers. In the figure, it appears that microseismicity is not uniform in this mass but it is divided into some smaller masses with high activity, as surrounded by dotted lines. On the other hand, Fig. 24 shows the topography of this raea, which may be divided into two parts, higher

(shadow part) and lower (white part) than 300 m. Rivers 1 to 4, are drawn in **Figs. 23** and **24**. We can recognize from these figures the fact that the rivers are situated nearly in the center of the smaller masses with high siesmicity. This means that microearthquakes occur in some cases along the rivers which divide the mountain mass, and that such rivres were not produced only by erosion, but they should have some tectonic significance. This result coincides with that mentioned in the previous section (3).

There are many examples to indicate that the existence of rivers appear to be related to microearthquake occurrences. **Fig. 25** shows distributions of microearthquakes and rivers in the vicinities of the Yamasaki fault and the ATL. Black parts in the figure represent the places with especially high seismicity. We can clearly recognize that some rivers have very close relation to microearthquake occurrence.

The distribution of microearthquakes along the Yamasaki fault is not an arrangement in a line in the strict sense. Microearthquakes appear to occur mostly at the intersection of the faults and the rivers, and such discrete small masses of microearthquake are aligned along the fault. The large and sharp offset of the Yamasaki

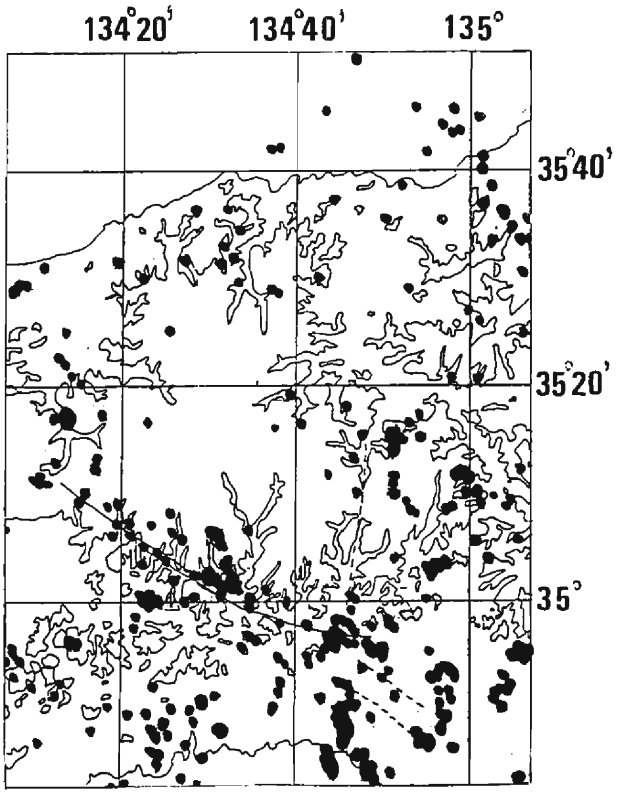

Fig. 22-a The Yamasaki fault system and microearthquakes around it are superimposed on the contours of 300 m

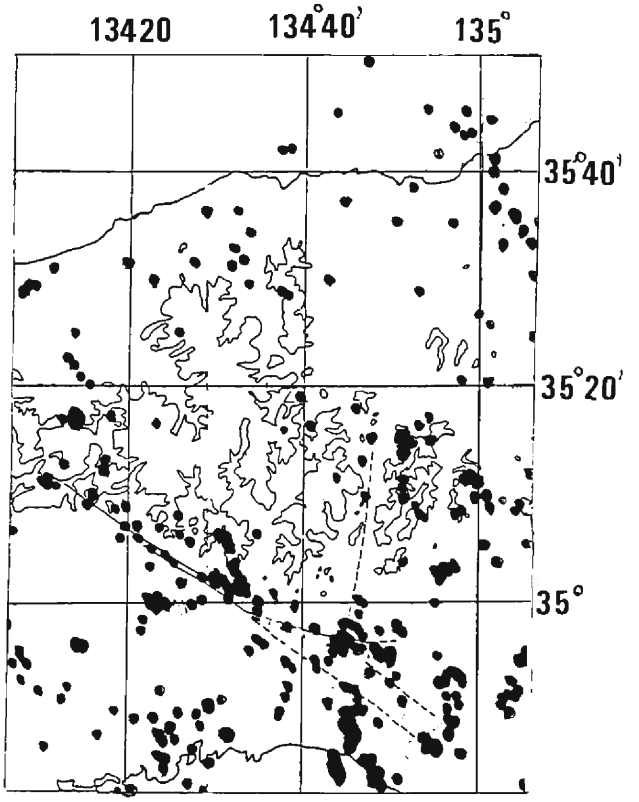

Fig. 22-b The same kind of figure as shown above, in which the contour indicates 600 m

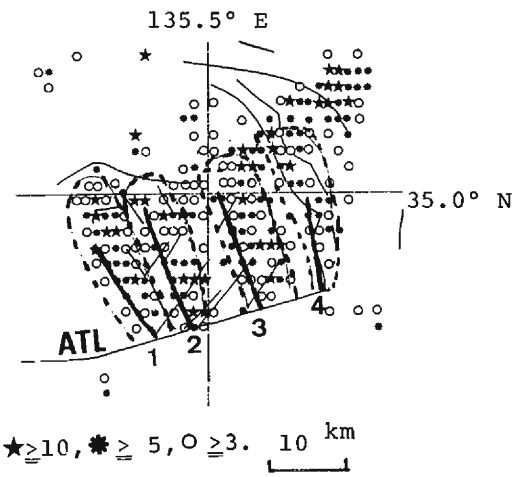

Fig. 23 Seismic activity in the north side of the ATL. Heavy lines, 1 to 4, perpendicular to the ATL correspond to short rivers.

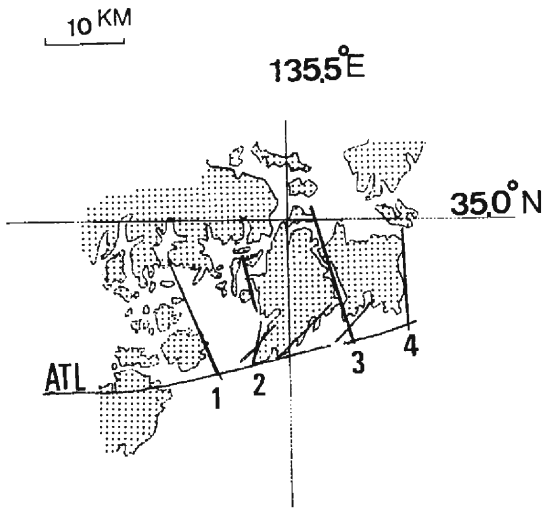

Fig. 24 Topography around the ATL. Contours indicate 300 m height and hatched area is higher than 300 m. The lines attached by numerals represent boundaries of blocks. These lines coinside with the rivers shown in Fig 23.

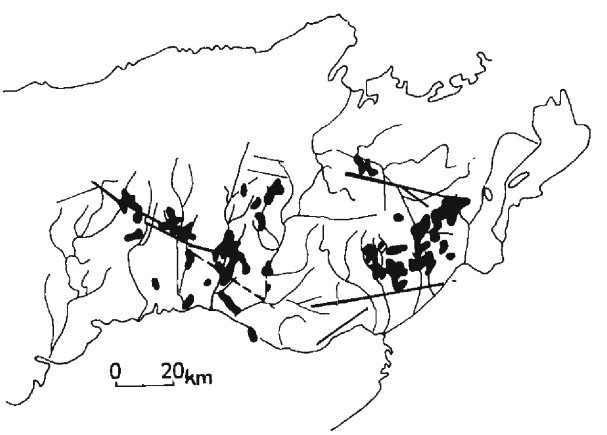

Fig. 25 Correlation between microearthquake occurrence and rivers. Dark areas and heavy lines indicate the area with especially high seismicity and main faults, respectively.

fault, which is recognized geomorphologically, is considered to have resulted from the large earthquakes, as described in 6.1.

7. Conclusions

1) The purpose of the present investigation is the following two items: The first one is to elucidate the formation mechanism of the topography which is considered

integration of the deformations on the Earth's surface produced by the tectonic stress over long geological time, and the second is to clarify a relationship between the present topography and earthquake occurrence which is the result from crustal activity produced by just the present tectonic stress.

2) In order to investigate various wavelengths topography in Southwest Japan, a two-dimensional Fourier analysis was applied to the Chubu district, the Inner Zone, the Outer Zone and the Kyushu district. The following results were obtained: There exist wavelengths longer than 40 km over the whole area. The pattern of two-dimensional spectra for the wavelengths around 40 km is different between the Inner Zone and Outer Zone, and the wavelengths seem to indicate large scale regionality. In the range of wavelength shorter than 30 km, there is large local difference in the spectra.

3) Referring to the above two-dimensional wavelength spectra, the topography with long wavelengths (the central wavelength, λ: 40 km and band width: 20–90 km), was extracted by the use of Seya's band-pass filter.

The topography with long wavelengths consists of one group of mountains with an EW strike in the Chugoku and Shikoku districts and of another group with an NS strike in the Chubu disttrict. Both the former and latter may be considered as a manifestation of fold topography relating to the whole crust. This interpretation seems consistent with the theories and experiments on folding. These two foldings might have been produced by NS and EW compressions from the Philippine Sea plate and the Pacific plate, respectively.

The Kinki district is situated between the above two groups, and has a topography with long wavelengths with an NE-SW strikes.

4) The topography with short wavelengths (λ: 20 km, band width: 10–40 km) extracted in the same manner as in the long wavelengths is more complicated and more regional pattern as compared with that with long wavelengths.

There exist two types of fold topographies with short wavelengths of an EW strike and an NS strike in the Chubu district and the Outer Zone. These may be considered to have been produced by the subductions of the Philippine Sea plate and of the Pacific plate, as in the case with long wavelengths.

The Chugoku and Kinki districts have complicated and irregulra patterns of topography in the range of short wavelengths.

If the topography with short wavelengths in this range is mainly related to the upper crust, the properties as well as the stress state in the upper crust in the Chugoku and Kinki districts may be different, to some extent, from those in Chubu district and the Outer Zone.

5) The topography with intermediate wavelengths (λ: 30 km, band width: 25–65 km) in the Chugoku district shows that the Chugoku mountains and Setouchi peneplain with an EW strike are superimposed by folding with an NS strike with intermediate wavelengths. This fact indicates that the Chugoku district has suffered double folding by both NS and EW compressions.

6) The characteristic topography in the Chugoku district indicates that rivers in this district flow straight northward or southward, and that the upper crust may have been divided into some blocks which have the uplift part of folding in it and are surrounded by rivers and tectonic lines. These features are almost the same in the Kinki district but appear more complicated, and many faults play an important role as the boundary.

7) The boundaries of these curstal blocks have tectonical origin. The structure of the Yamasaki fault, one example of such boundaries, was investigated from several viewpounds, earthquake occurrence, ground water and apparent electrical resistivity of rock. From these results, the Yamasaki fault is considered as a crushed zone with considerable widths which depend on the kinds of observations.

8) Most large earthquakes have occurred at the boundary between two regions of uplift and subsidence of fold topography, especially of short wavelengths (λ: 20 km). This may be due to generation of faults at the boundary along with the development of the fold.

9) Occurrence of microearthquakes shows good correlations to topography with long wavelengths as well as to fine structures.

The fact that microearthquakes are distributed along the boundary between the uplift and subsidence parts of the fold shows the existance of faults there.

10) Correlations of microearthquake occurrence to small structures is extended from the topography of very short wavelengths (λ: 16 km) to actual landforms of small dimensions. Rivres, and sharp notches of the contour appear to have some relations with microearthquake occurrences along them. These facts indicate that such fine landforms have a tectonic setting extending down to the deepest foci of microearthquakes around 15 km.

Acknowledgements

I would like to express sincere thanks to Professors Yoshimichi Kishimoto and Kauzo Oike for their continuous guidance and encouragement throughout this study and criticla reading of manuscript. I am very gratefull to Professor Emeritus Sadao Sasajima for his kind instructions in geological and geomorphological problems, especially relating to this work. I am indebted also to Professor Norihiko Sumitomo for his valuable advice and critical reading of manuscript. Thanks are also given to colleagues of the Microearthquake Research Section for their discussions and suggestions. Especially, Mr. Kzauo Matsumura gave helpfull suggestions on computation in this study and thanks are due to the Abuyama Seismological Observatory for the use of the data of microearthquake epicenters. The numerical computations were performed by using the **FACOM M-140** computer at the Data Processing Center, Disaster Prevention Research Institute, Kyoto University.

References

1) Mino, K.: Relation between topography and seismicity —Stress field of Japanese Islands—, Zisin, 34, 1981, pp. 213–222.
2) Mino, K. and K. Matsumura: Topography and earthquakes —Slope of topography and earthquakes—, Disaster Prev. Res. Inst. Annuals, Kyoto Univ., 25–B–1, 1982, pp. 47–57.
3) Davis, M.W.: The Geographical Cycle, Geogr. Jour., 14, 1899, pp. 481–430.
4) Tsujimura, T.: The Goemorphology, Kokin Shoin, 1923.
5) Otsuka, Y.: Active rock folding in Japan, Proc. Imp. Acad. Japan, 17, 1941, pp. 518–522.
6) Sugimura, A.: On the deformation of the Earth's surface owing to the rock folding in Japan, Bull. Earthq. Res. Inst., 30–2, 9152, pp. 163–178.
7) Kaizuka, S.: Undulatory crustal deformation of upper Pleistocene terrace in Japan, Geogr. Studies, Prof. Tsujimura, 1961, pp. 119–131.
8) Matsuda, T.: Rate of folding in late Tertiary and Quaternary in Japan, Proc. U.S.-Japan Conference, Earthq. Prediction, Problem, 1964, pp. 96–98.
9) Ota, Y.: Crustal movements in the late Quaternary considered from the deformed terrace plains in Northeast Japan, Jour. Geol. Geogr. Japan, 40, (2–4), 1969, pp. 41–61.
10) Miyamura, S. and M. Mizoue: Secular vertical movements of the earth's crust in Japan, Geod. Soc. Japan, 10, 1964, pp. 123–138.
11) Kaizuka, S.: Distribution of Quaternary fold, especially in rate and axis direction in Japan, Geogr. Rept. Tokyo Metropl. Univ., 3, 1968, pp. 1–9.
12) Mizoue, M.: Relation between crustal structures and crustal movement in Japan, Jour. Geogr., 73, 1964, pp. 224–242.
13) Yoshikawa, T.: Prof. N. Yamasaki's Contribution to Tectonic Geomorphology, Geogr. Rev. Japan, 44, 8, 1971, pp. 552–564.
14) Kuno, H.: On the displacement of the Tanna Fault since the Pleistocene, Bull. Earthq. Res. Inst., 14, 1936, pp. 621–631.
15) Matsuda, T.: Strike-slip Faulting along the Atotsugawa Fault, Japan, Bull. Earthq. Res. Inst. 44, 1966, pp. 1179–1212.
16) Sugimura, A. and T. Matsuda: Atera fault and its displacement vectors, Bull. Geol. Soc. Amer., 76, 1965, pp. 509–522.
17) Matsuda, T. and M. Okada: Studies of active faults in Japan, Quaternary Res., 7, 1968, pp. 188–199.
18) Okada, M.: On the Quaternary faulting along the Median Tectinic Line, "Median Tectonic Line", Tokai Univ. press, 1973, pp. 49–86.
19) Huzita, K., Y. Kishimoto and K. Shiono: Neotectonics and seismicity in the Kinki area, Southwest Japan, Jour. Geosci. Osaka City Univ., 16, 1973, pp. 93–124.
20) Matsuda, T.: Magnitude and Recurrence Interval of Earthquakes from a fault, Zisin, 2, 18, 1975, pp. 269–283.
21) Clement, W.G.: Basic principles of two-dimensional digital filtering, Geophys. Prosp., 1972, pp. 125–145.
22) Seya, K.: On the New Metohd of Analysis in Gravity Prospecting, Geol. Surv. Japan, Rept. 201, 1963.
23) Willis, B.: The mechanics of *Appalachian* structure, 13′ Ann. Rept. U.S. Geol. Surv., 1893, pp. 211–281.
24) Smoluchowksi, M.: Über ein gewisses Stabilitts problem der Elastizitatslehre und der Zbeziehungen zur Entstehung von Flatenbirgen, Anz. Akad. Wiss. Krkau, Math. Naturw., 2: 3 1909.
25) Smoluchowksi, M.: Some remarks on the mechanics of overthrusts, Geol. Mag., 6, 1909, pp. 204–205.
26) Bito, M.A.: Folding instability of a layered viscoelastic medium under compression, Proc. R. Soc. London, Ser. A, 242, 1957, pp. 444–454.
27) Biot, M.A.: Theory of folding of stratified viscoelastic media and its implications in tectonic and orogenesis, Geol. Soc. Amr. Bull., 72, 1961, pp. 1595–1620.

28) Ramberg, H.: Fluid dynamics of viscous buckling applicable to folding of layered rocks, Bull. Amr. Assoc. Petr. Geol., 47, 1963, pp. 484–505.
29) Sherwin, J.A. and W.M. Chapple: Wavelengths of single layer folds: A comparison between theory and observation, Amr. Jour. Sci., 2, 266, 1968, pp. 167–179.
30) Hudleston, P.J.: An analysis of "Single layer" folds developed experimentally in viscous media, Tectonophys. 16 (3/4), 1973, pp. 189–214.
31) Naruse, Y.: Rates of crustal movement in Boso Peninsula during the late Cenozoic, Bull. Osaka Univ. Eocnomics, 80, 1971, pp. 228–245.
32) Ota, Y. and T. Yoshikawa: Regional characteristics and their geodynamic implidations of late Quaternary tectonic movement deduced from deformed former shorelines in Japan, Jour. Phys. Earth, 26, Suppl., 1978, pp. 379–389.
33) Huzita, K.: Tectonic development of Southwest Japan in the Quaternary period, Jour. Geosci. Osaka City Univ. 12, 1969, pp. 53–70.
34) Chapman, M.E. and Solomon, S.C.: North America-Eurasian Plate Boundary in Northeast Asia, Jour. Geophys. Res., vol. 81, No. 5, 1976, pp. 921–930.
35) Huzita, K.: Role of the Median Tectonic Line in the Quaternary tectonics of the Japanese Islands, Mem. Geol. Soc. Japan, No. 18, 1980, pp. 129–153.
36) Takeuchi, A.: The Pliocene stress field and tectonism in the Shin-Etsu region, central Japan, Jour. Geosci. Osaka City Univ. Vol. 21, 1978, pp. 37–52.
37) Kanamori, H.: Tectonic implications of the 1944 Tonankai and the 1946 Nankaido earthquakes, Phys. Earth Planet. Interiors 5, 1972, pp. 129–139.
38) Seto, T.: The instantaneous rotation vector of the Philippine Sea plate relative to the Eurasian plate, Tectonophys. 42, 1977, pp. 209–226.
39) Shiono, K.: Focal mechanism of small earthquakes in the Kii peninsula, Kii channel and Shikoku, Southwest Japan and some problems related to the Plate Tectonics, Jour. Geosci. Osaka City Univ., 16, 1973, pp. 69–91.
40) Okano, K., M. Nakmaura, T. Konomi and S. Kimura: Recent Seismic Activities along the Nankai Trough off Southwest Japan in Relation to Major Earthquakes, Mem. Fac. Sci. Kochi Univ., Vol. 4, Ser. B, 1983, pp. 1–10.
41) Hurukawa, N.: Upper-Mantle Structure in the Kinki District, Japan as revealed by Apparent Velocities of Subcrustal Earthquakes in the Kii Peninsula, Jour. Phys. Earth, 31, 1983, pp. 47–64.
42) Nakanishi, I.: Percursors to ScS phases and dipping interface in the upper mantle beneath Southwest Japan, Tectonophys. 69, 1980, pp. 1–35.
43) Kuno, H.: Lateral variation of basalt magma type across continental margins and island arcs, Bull. Volcanol., 29, 1966, pp. 192–222.
44) Hirahara, K.: Three-Dimensional Seismic Structure bneath Southwest Japan: The Subducting Philippine Sea Plate, Tectonophys., 79, 1981, pp. 1–44.
45) Kambe, N. and Hirokawa, O.: SAYO-explanatory text of the gelogical map of Japan (1/50,000 scale), Geol. Surv. Japan, 1963.
46) Geological Survey of Japan.: MINES SUMMARY REPORT, Rept. 260, vol. 2., 1980.
47) Geographical Survey Institute: Reports of 1'st order leveling surveys, suppl. Vol. 1–5, 1972–1976.
48) Nakane, K.: Horizontal Tectonic Strain in Japan, part 1 and 2, Jour. Geod. Soc., Japan, 19–4, 1973, pp. 190–208.
49) Ichikawa, M.: Reanalyses of Mechanism of Earthquakes which Occurred in and near Japan, and Statistical Studies on the Nodal Plane Solutions Obtained, 1926–1968, Geophys. Mag., 35–3, 1971, pp. 207–274.
50) Okuda, S.: Successive erosion by water and ice in Japan, Kagaku-Asahi, 1979, (in Japanese)
51) The Research Group for Active Faults: ACTIVE FAULTS IN JAPAN, Tokyo Univ. Press, 1980.
52) Oike, K.: Spatial and temporal distribution of mirco-earthquakes and active faults, Mem. Geol. Soc. Japan., 12, 1976, pp. 59–73.

53) Oike, K. and Y. Kishimoto: The Yamasaki fault as a test-field for earthquake prediction, Proc. Earthq. Prediction, Proc. Earthq. Prediction Res. Symposium (1976) 1976, pp. 83–90.
54) Handa, S. and N. Sumitomo: MT sounding around active fault by using natural electromagnetic noises in the ELF range —Yamasaki fault—, Tsukumo Earth, Sci., 14, 1979, pp. 21–31.
55) Yoshioka, R.: Relation between Chloride ion content in Shiota hot spring near the Yamasaki fault and small earthquakes in its vicin·ty, Proc. Earthq. Prediction Res. Symposium (1980), 1980, pp. 159–162.
56) Wakita, H., Y. Nakamura, I. Kita, N. Fujii and K. Notsu: Hydrogen release: New indicater of fault activity, Science, 210, 1980, pp. 188-190.
57) Electromagnetic Research Group for the Active Fault.: Low Electrical Resistivity along an Active Fault, Jour. Geomag. Geoelect., 34, 1982, pp. 103–217.
58) Mino, K.: Distribution of underground water around Yamasaki fault (1) —Observation at Yasutomi Region—, Zisin, 2–33, 1980, pp. 117–130.
59) Usami, T.: Damaging Earthquakes in Japan, Tokyo Univ. press, 1975.
60) Tokyo Astronomical Observatory: "Rika-Nenpyo" in Japanese, Maruzen Press., 1982.
61) Japan Meteorological Agency (JMA): Catalogue of Major Earthquakes which occurred in and near Japan. (1926–1956).
62) Utsu, T.: Seismicity of Japan from 1885 through 1925 —A New Catalog of Earthquakes of M 6 Felt in Japan and Smaller Earthquakes Which Caused Damage in Japan—, Bull. Earthq. Res. Inst., Vol. 54., 1979, pp. 253–308.
63) Wiltschko, D.V.: Partitioning of energy in a thrust sheet and implication concerning driving forces, Jour. Geophys. Res. 84, 1979, pp. 6050.
64) Brace, W.: State of stress in the earth's crust, W. Judd, eds., in Brittle Fracture of Rocks, Elsevier publisher., 1963.
65) McKenzie, D.P.L: The realtion between fault plane solutions for earthquakes and the directions of the principal stresses, Bull. Seim. Soc. Amer., vol. 59–2, 1969, pp. 591–601.
66) Huzita, K.: Rokko mountains, and its appearance, Quaternary Res., 7, 1968, pp. 248–260.
67) Sangawa, A.: Geomorphic Development and Crustal Movement of The Middle Course Basin of The Kinokawa River, Geogr. Rev., Japan, 50, 1977, pp. 578–595.
68) Kishimoto, Y., K. Oike, K. Watanabe, T. Tsukuda, N. Hirano and S. Nakao: On the Telemeter Observation System of the Tottori and Hokuriku Micro-earthquake Observatory, Zisin, 2–31, 1978, pp. 265–274.
69) Kuroiso, A. and H. Watanabe: On the Telementered Array System for Microearthquake Observation at Abuyama Seismological Observatory, Zisin, 2–30, 1977, pp. 91–106.
70) Wada, H., T. Mikumo and M. Koizumi: Seismicity and focal mechanism of local earthquakes along the Atotsugawa fault and in the Northern Hida Region, Zisin, 2–32, 1979, pp. 281–296.